Numerical analytic continuation of Euclidean data

Ralf-Arno Tripolt, ECT*, Trento, Italy

Based on arXiv: 1610.03252

Ralf-Arno Tripolt, Idan Haritan, Jochen Wambach, Nimrod Moiseyev

'Hadrons under extreme conditions', COST - THOR Working Group 1 Meeting

Swansea, September 12th-14th, 2017

ECT*

EUROPEAN CENTRE FOR THEORETICAL STUDIES
IN NUCLEAR PHYSICS AND RELATED AREAS

Outline

I) Introduction

- rational interpolants
- Schlessinger Point Method (SPM)
- Thiele's interpolation function (TIF)

II) Applications

- simple examples
- extraction of complex resonance poles and decay thresholds
- analytic continuation - from imaginary to real time
- direct comparison of numerical analytic continuation methods

III) Summary

I) Introduction

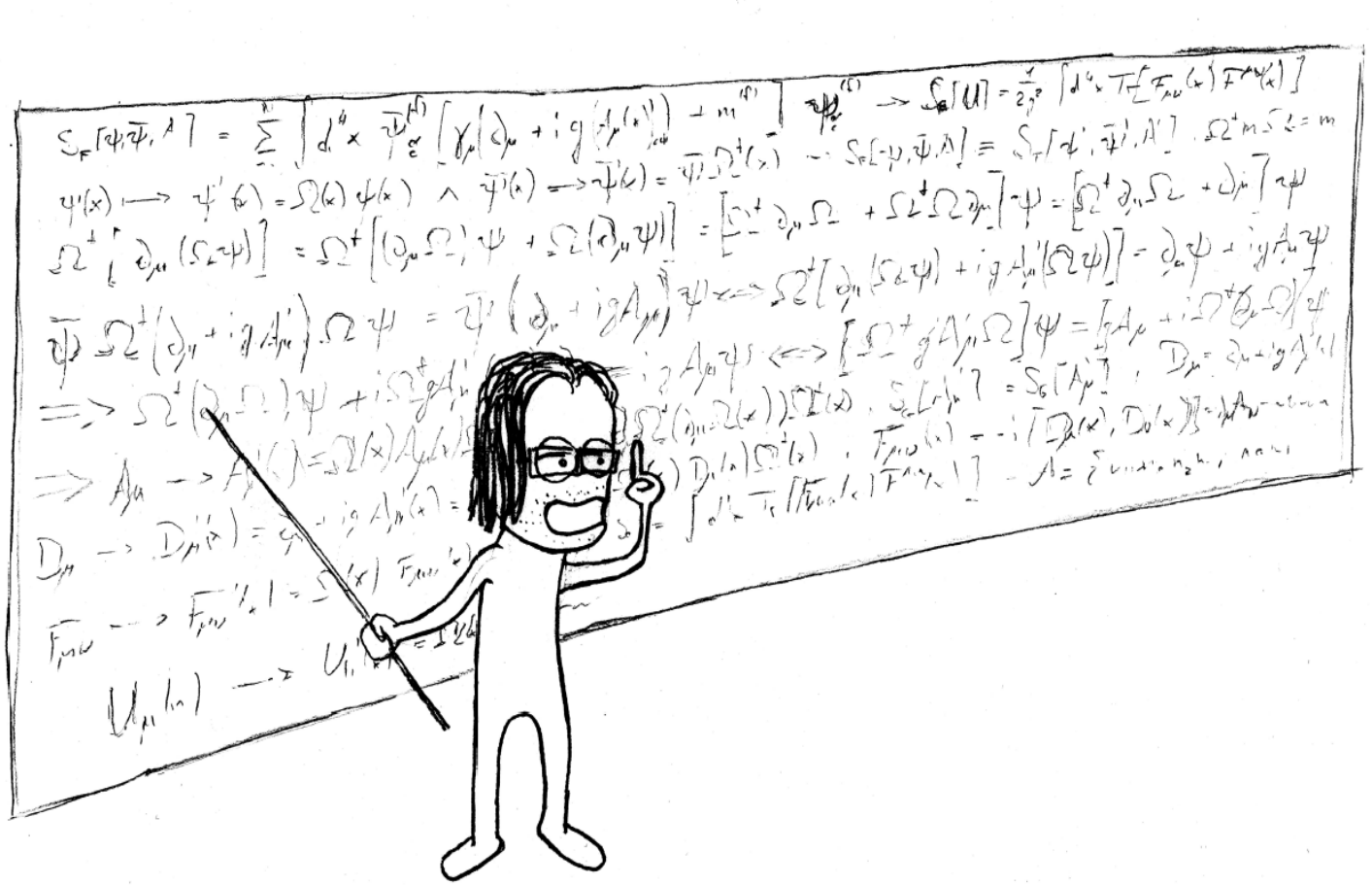

[courtesy L. Holicki]

Rational Interpolants

- rational interpolants are defined in such a way that they reproduce a given data set of real or complex points (x_i, f_i)
- the rational interpolant $p(x)/q(x)$ with polynomials $p(x) = \sum_{i=0}^{m} a_i x^i$ of order m and $q(x) = \sum_{i=0}^{n} b_i x^i$ of order n fulfills

$$f(x_i) = \frac{p(x_i)}{q(x_i)}, \qquad i = 1, \ldots, m+n+1$$

- the coefficients a_i and b_i of the polynomials $p(x)$ and $q(x)$ can be determined by solving the homogeneous system of $m+n+1$ linear equations for the $m+n+2$ unknown coefficients,

$$f(x_i)q(x_i) = p(x_i), \qquad i = 1, \ldots, m+n+1$$

- we choose $q(0) = 1$

[J. Kallrath, *On Rational Function Techniques and Padé Approximants. An Overview.* (2002)]
[G.A. Baker, *Essentials of Padé Approximants*, Academic Press, New York, (1975)]
[G.A. Baker and J.L. Gammel, *The Padé Approximant in Theoretical Physics*, Academic Press, New York, (1970)]
[G.A. Baker, Advances in Theoretical Physics, Academic Press, New York, (1965)]
[H.S. Wall, *Analytic Theory of Continued Fractions*, Chelsea, New York, (1948)]

Rational Interpolants

- the rational interpolants along the upper main staircase with $m = n$ or $m = n - 1$ can be obtained by the Schlessinger point method (SPM)
- the rational interpolants along the lower main staircase with $m = n$ or $m = n + 1$ can be obtained by Thiele's interpolation formula (TIF)

$m \backslash n$	0	1	2	3
0	$\frac{1}{1}$	$\frac{1}{1-z}$	$\frac{1}{1-z+\frac{1}{2}z^2}$	$\frac{1}{1-z+\frac{1}{2}z^2-\frac{1}{6}z^3}$
1	$\frac{1+z}{1}$	$\frac{1+\frac{1}{2}z}{1-\frac{1}{2}z}$	$\frac{1+\frac{1}{3}z}{1-\frac{2}{3}z+\frac{1}{6}z^2}$	$\frac{1+\frac{1}{4}z}{1-\frac{3}{4}z+\frac{1}{4}z^2-\frac{1}{24}z^3}$
2	$\frac{1+z+\frac{1}{2}z^2}{1}$	$\frac{1+\frac{2}{3}z+\frac{1}{6}z^2}{1-\frac{1}{3}z}$	$\frac{1+\frac{1}{2}z+\frac{1}{12}z^2}{1-\frac{1}{2}z+\frac{1}{12}z^2}$	$\frac{1+\frac{2}{5}z+\frac{1}{20}z^2}{1-\frac{3}{5}z+\frac{3}{20}z^2-\frac{1}{60}z^3}$
3	$\frac{1+z+\frac{1}{2}z^2+\frac{1}{6}z^3}{1}$	$\frac{1+\frac{3}{4}z+\frac{1}{4}z^2+\frac{1}{24}z^3}{1-\frac{1}{4}z}$	$\frac{1+\frac{3}{5}z+\frac{3}{20}z^2+\frac{1}{60}z^3}{1-\frac{2}{5}z+\frac{1}{20}z^2}$	$\frac{1+\frac{1}{2}z+\frac{1}{10}z^2+\frac{1}{120}z^3}{1-\frac{1}{2}z+\frac{1}{10}z^2-\frac{1}{120}z^3}$
4	$\frac{1+z+\frac{1}{2}z^2+\frac{1}{6}z^3+\frac{1}{24}z^4}{1}$	$\frac{1+\frac{4}{5}z+\frac{3}{10}z^2+\frac{1}{15}z^3+\frac{1}{120}z^4}{1-\frac{1}{5}z}$	$\frac{1+\frac{2}{3}z+\frac{1}{5}z^2+\frac{1}{30}z^3+\frac{1}{360}z^4}{1-\frac{1}{3}z+\frac{1}{30}z^2}$	$\frac{1+\frac{4}{7}z+\frac{1}{7}z^2+\frac{2}{105}z^3+\frac{1}{840}z^4}{1-\frac{3}{7}z+\frac{1}{14}z^2-\frac{1}{210}z^3}$

[L. Schlesinger, Physical Review, Volume 167, Number 5 (1968)]
[R.W. Haymaker and L. Schlesinger, Mathematics in Science and Engineering, Volume 71, Chapter 11 (1970)]
[M. Abramowitz and I.A. Stegun,*Handbook of Mathematical Functions*, New York, Dover, (1972)]
[L.M. Milne-Thomson, *The Calculus of Finite Differences*, London, Macmillan, (1951)]

Schlessinger Point Method (SPM)

Given a finite set of $N = m + n + 1$ data points (x_i, f_i) we construct the rational interpolant $p(x)/q(x)$ with polynomials $p(x)$ of order m and $q(x)$ of order n that is given by the continued fraction

$$p(x)/q(x) = C_N(x) = \cfrac{f_1}{1 + \cfrac{a_1(x - x_1)}{1 + \cfrac{a_2(x - x_2)}{1 + \cfrac{}{\vdots a_{N-1}(x - x_{N-1})}}}},$$

where the coefficients a_i are given recursively by $a_1 = \frac{f_1/f_2 - 1}{x_2 - x_1}$ and

$$a_i = \frac{1}{x_i - x_{i+1}} \left(1 + \frac{a_{i-1}(x_{i+1} - x_{i-1})}{1+} \frac{a_{i-2}(x_{i+1} - x_{i-2})}{1+} \cdots \frac{a_1(x_{i+1} - x_1)}{1 - f_1/f_{i+1}} \right)$$

[L. Schlessinger, Physical Review, Volume 167, Number 5 (1968)]
[R.W. Haymaker and L. Schlesinger, Mathematics in Science and Engineering, Volume 71, Chapter 11 (1970)]
[H.J. Vidberg and J.W. Serene, Journal of Low Temperature Physics, Vol. 29, Nos. 3/4 (1977)]
[A. Pilaftsis and D. Teresi, Nucl. Phys. B 874 (2013) 594-619]
[G. Markó, U. Reinosa and Z. Szép, arXiv: 1706.08726]

Thiele's Interpolation Function (TIF)

Given a finite set of $N = m + n + 1$ data points (x_i, f_i) we construct the rational interpolant $p(x)/q(x)$ with polynomials $p(x)$ of order m and $q(x)$ of order n that is given by the continued fraction

$$T_N(x) = f_1 + \cfrac{x - x_1}{\rho_1(x_1, x_2) + \cfrac{x - x_2}{\rho_2(x_1, x_2, x_3) - f_1 + \cfrac{x - x_3}{\rho_3(x_1, x_2, x_3, x_4) - \rho_1(x_1, x_2) + \ldots}}}$$

where the reciprocal differences are given by

$$\rho_1(x_1, x_2) = \frac{x_1 - x_2}{f_1 - f_2},$$

$$\rho_2(x_1, x_2, x_3) = \frac{x_1 - x_3}{\rho_1(x_1, x_2) - \rho_1(x_2, x_3)} + f_2,$$

$$\rho_n(x_1, x_2, \ldots, x_n) = \frac{x_1 - x_n}{\rho_{n-1}(x_1, \ldots, x_{n-1}) - \rho_{n-1}(x_2, \ldots, x_n)} + \rho_{n-2}(x_2, \ldots, x_{n-1})$$

[M. Abramowitz and I.A. Stegun, *Handbook of Mathematical Functions*, New York, Dover, (1972)]
[L.M. Milne-Thomson, *The Calculus of Finite Differences*, London, Macmillan, (1951)]

SPM and TIF - general properties

- the SPM gives a rational interpolant of order $(n, n+1)$ for an even number of input points and (n, n) for an odd number of input points
- the TIF gives a rational interpolant of order $(n, n-1)$ for an even number of input points and (n, n) for an odd number of input points
- SPM and TIF are identical for an odd number of input points
- any knowledge on the large-distance behavior of the underlying function may be used to choose the order of the rational interpolant

Analytic Continuation and Radius of Convergence

- an analytic continuation into the complex plane can be performed by choosing x in $C_N(x)$ or $T_N(x)$ to be complex, i.e. $x = \alpha e^{i\theta}$
- rational interpolants can exactly reproduce polar singularities, thus extending the 'radius of convergence' to the first non-polar singularity, e.g. a branch point
- even non-polar singularities may be well approximated by poles and zeros of the rational fraction
- a rational fraction can have only one sheet in the complex plane - a many-sheeted function can only be reconstructed on a single sheet

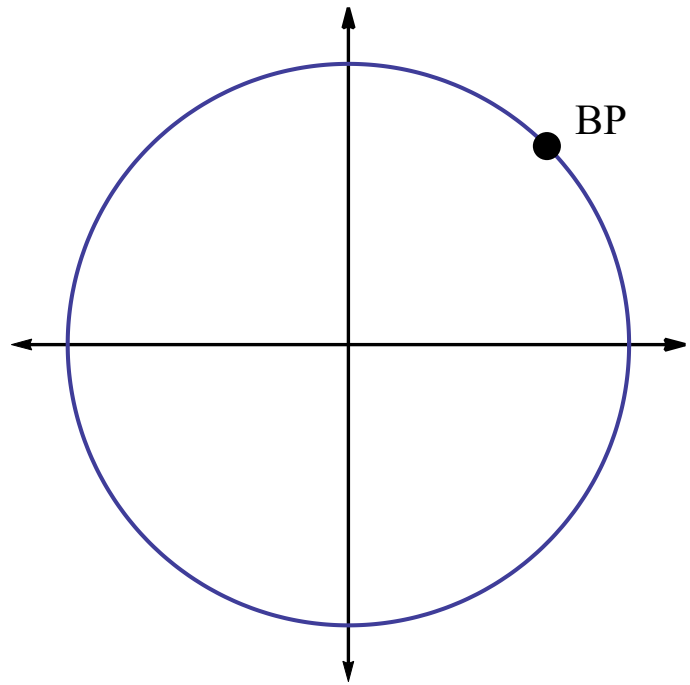

Rational Approximants - N=2

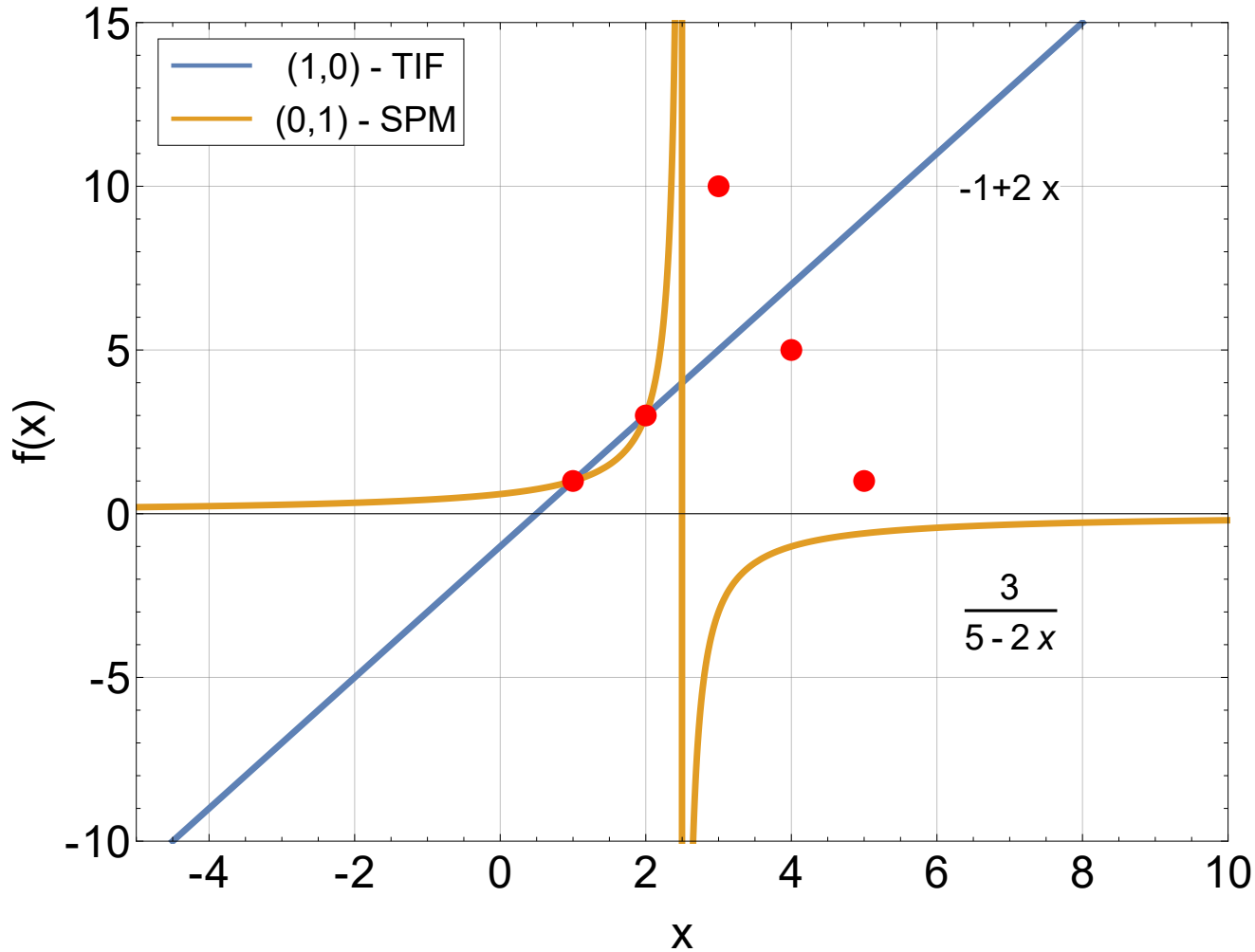

Rational Approximants - N=3

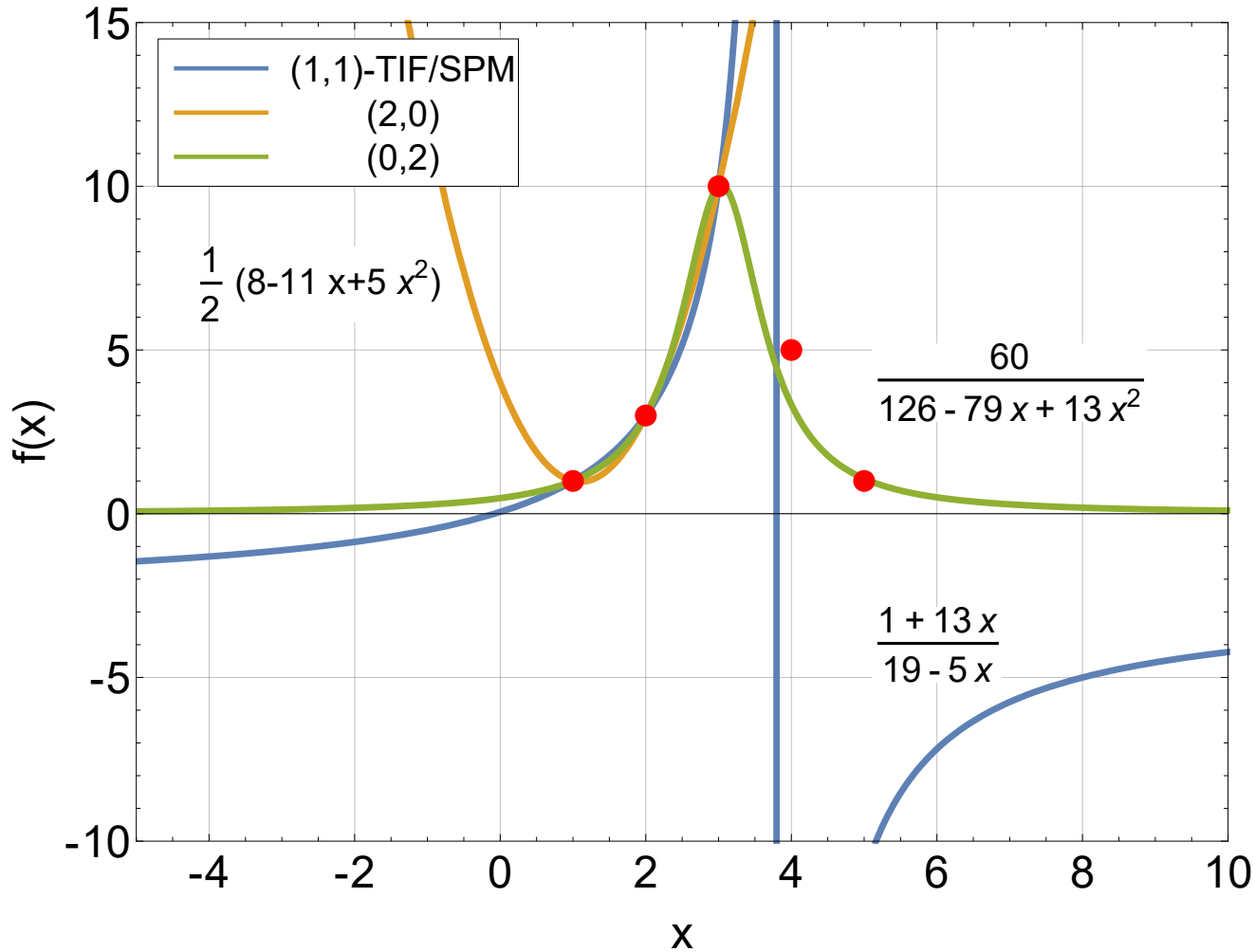

Rational Approximants - N=4

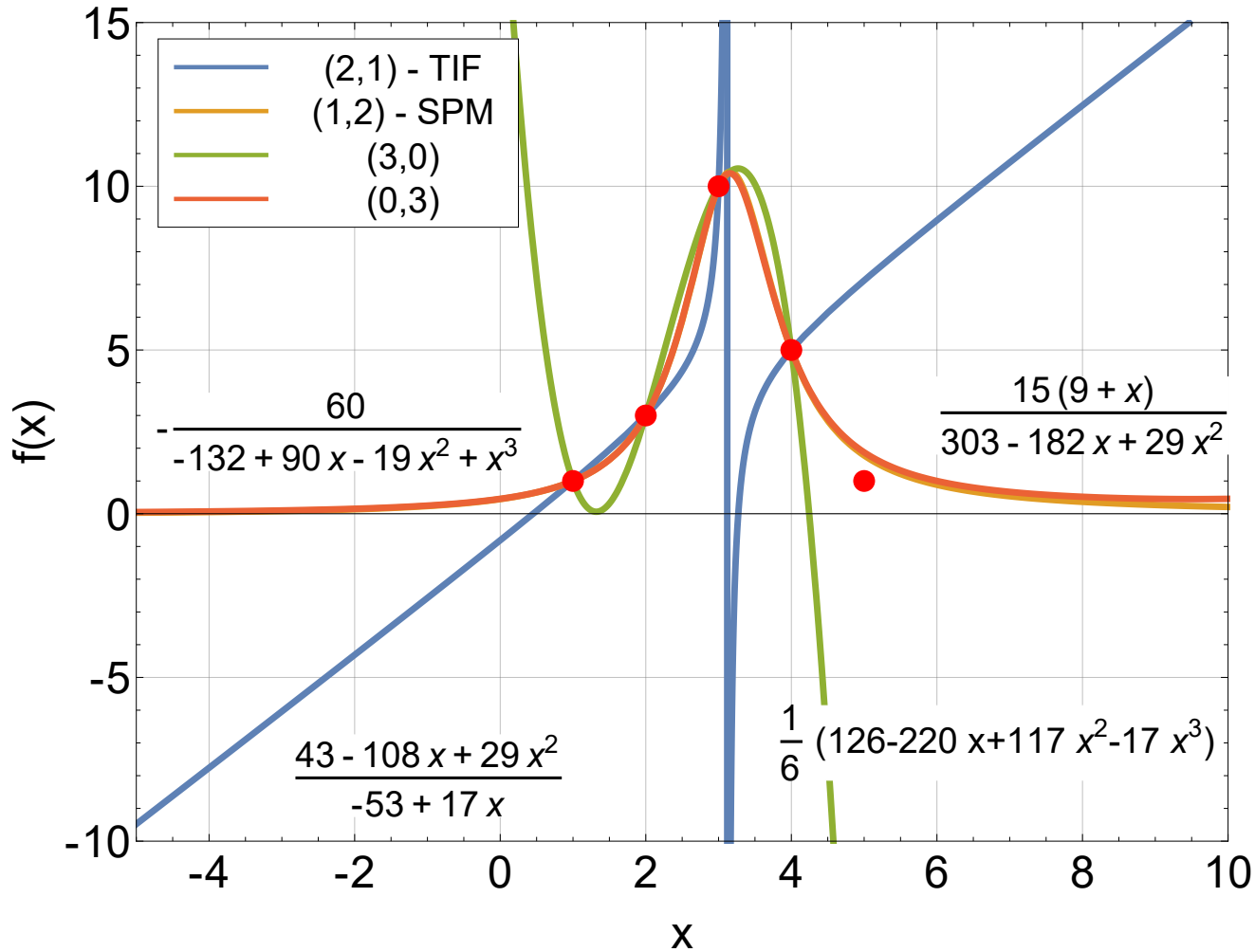

Rational Approximants - N=5

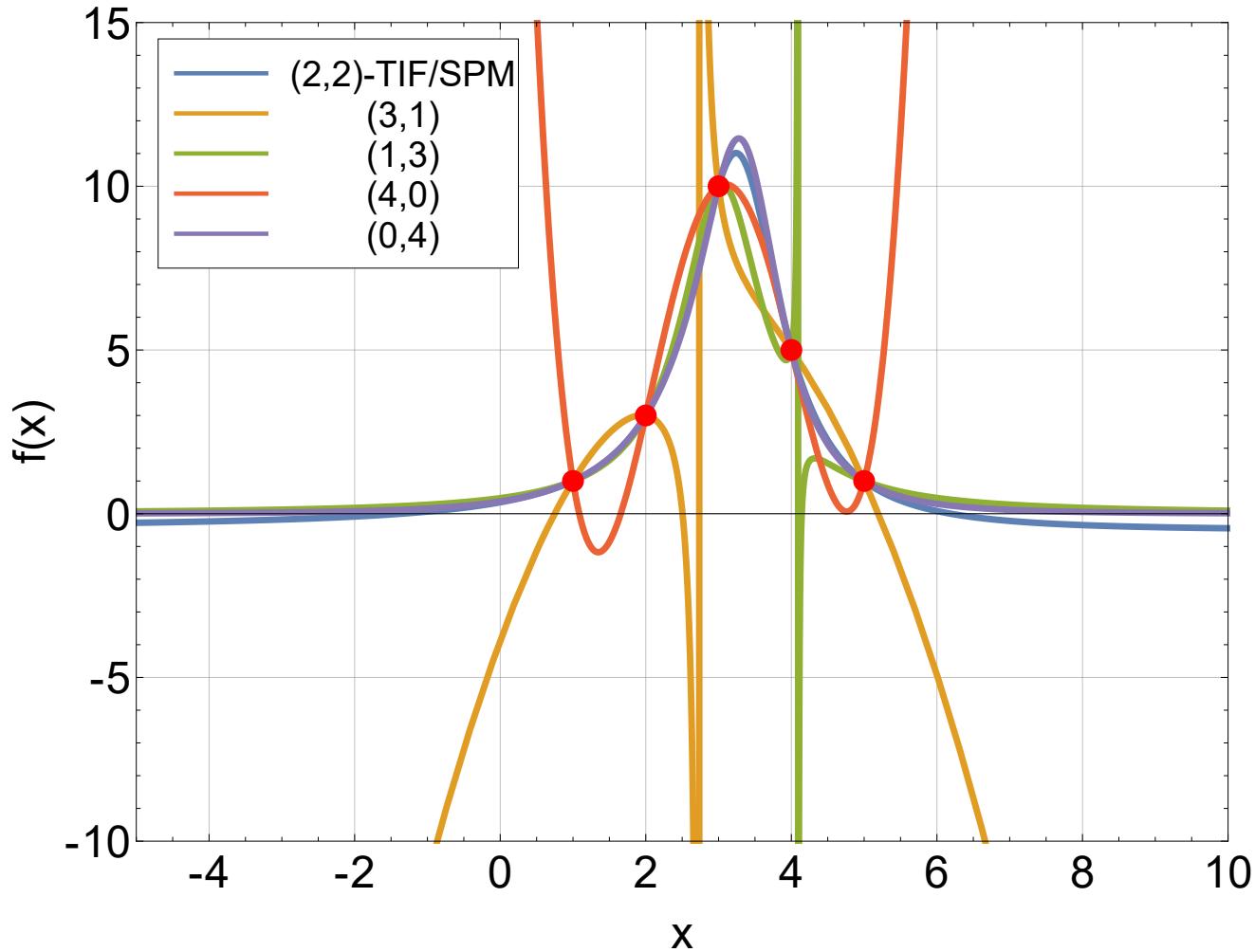

II) Applications

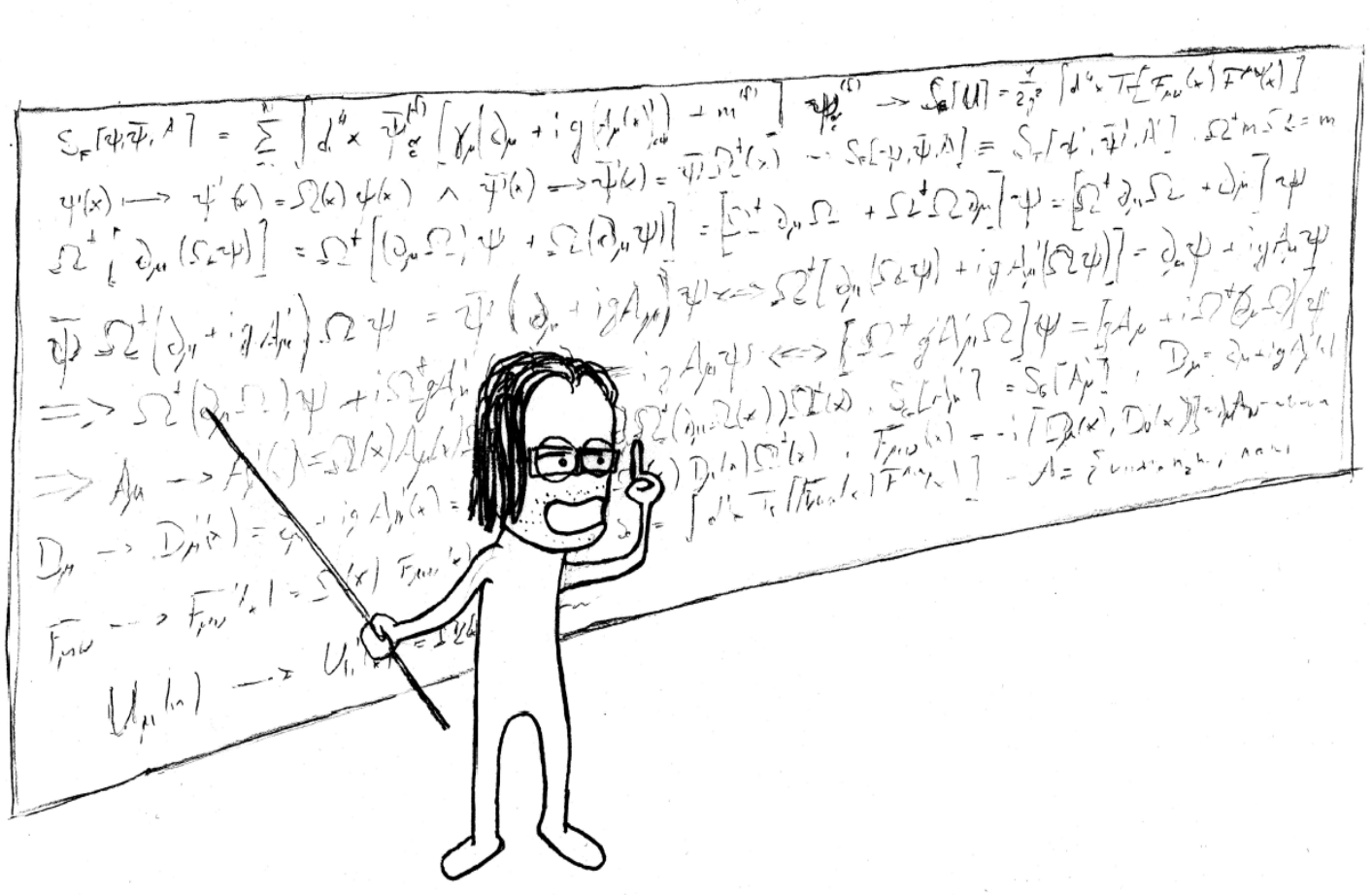

[courtesy L. Holicki]

Extrapolation of $f(x) = e^x$

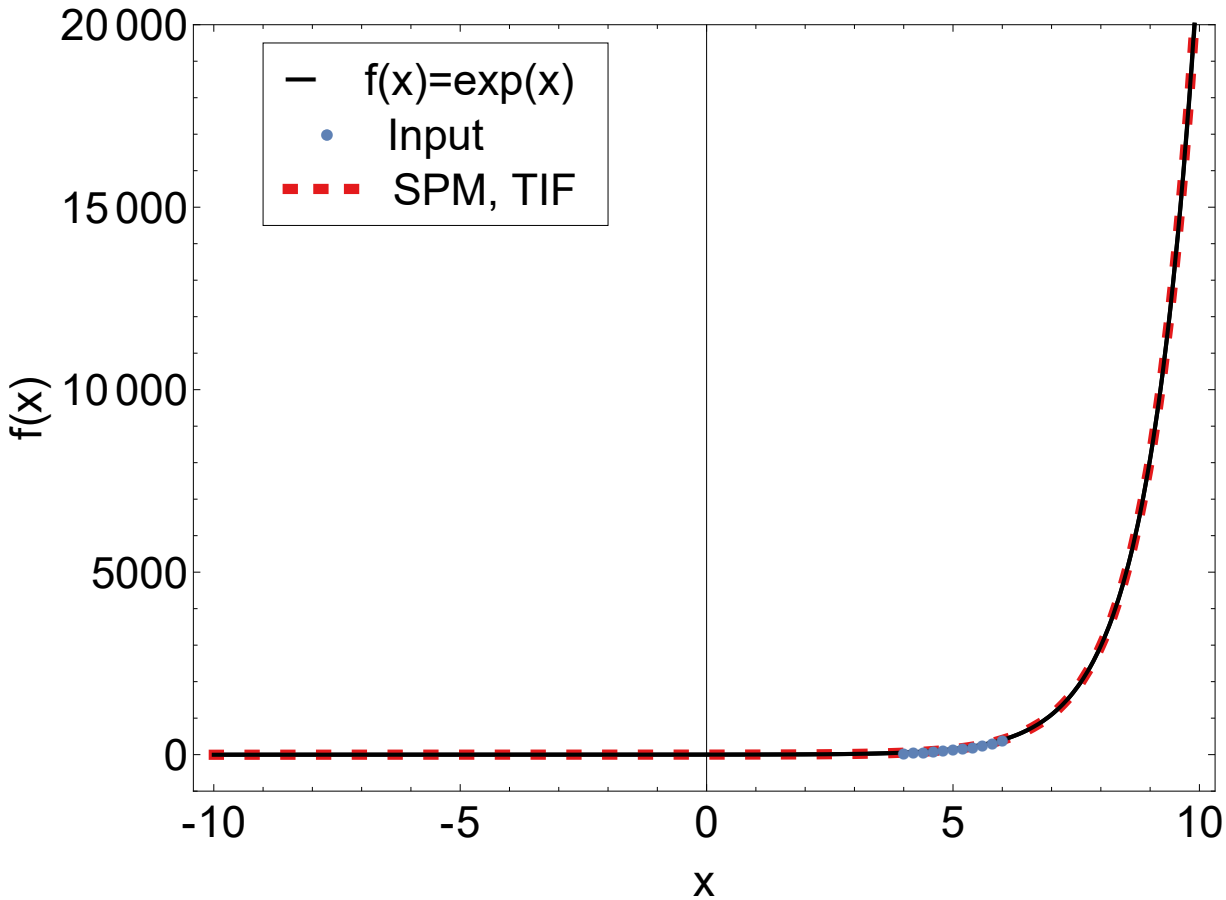

- for $N = 11$ one obtains

$$C_N(x) = T_N(x) = \frac{263504 + 170536\,x + 46451\,x^2 + 10389\,x^3 + 756\,x^4 + 148\,x^5}{265568 - 98809\,x + 15473\,x^2 - 1274\,x^3 + 55\,x^4 - x^5}$$

Extrapolation of $f(x) = e^x$

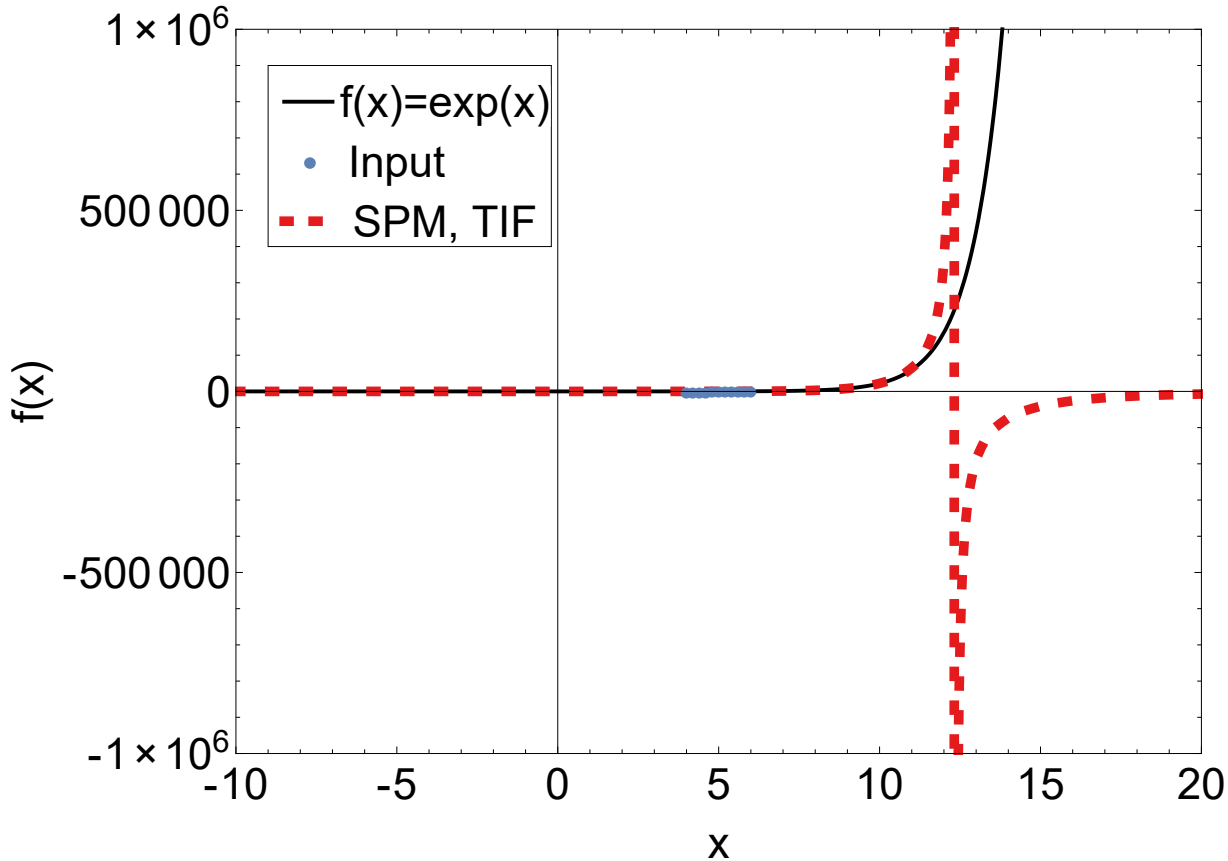

- for $N = 11$ one obtains

$$C_N(x) = T_N(x) = \frac{263504 + 170536\,x + 46451\,x^2 + 10389\,x^3 + 756\,x^4 + 148\,x^5}{265568 - 98809\,x + 15473\,x^2 - 1274\,x^3 + 55\,x^4 - x^5}$$

Analytic Continuation of $f(x) = e^x$

Re $\exp(x)$:

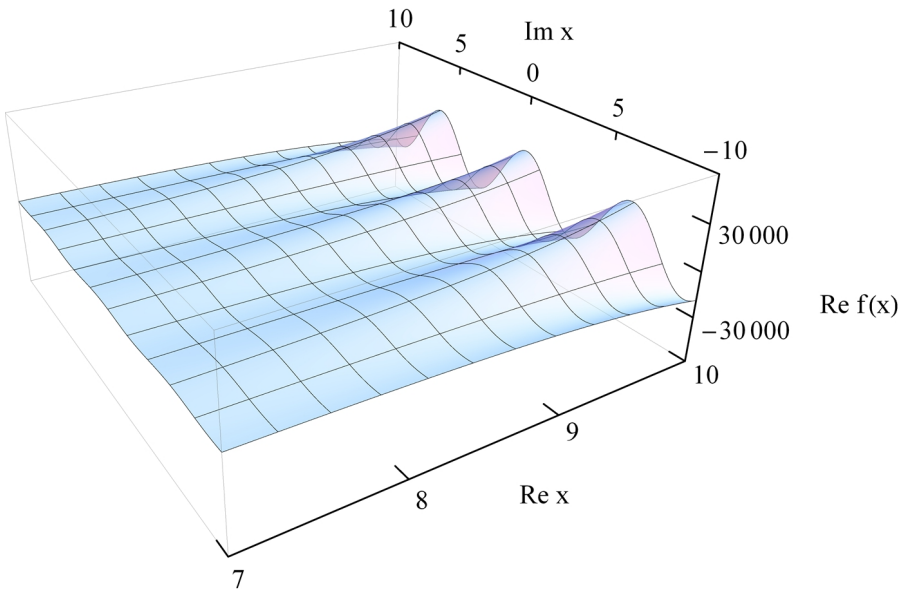

Re $C_N(x)$:

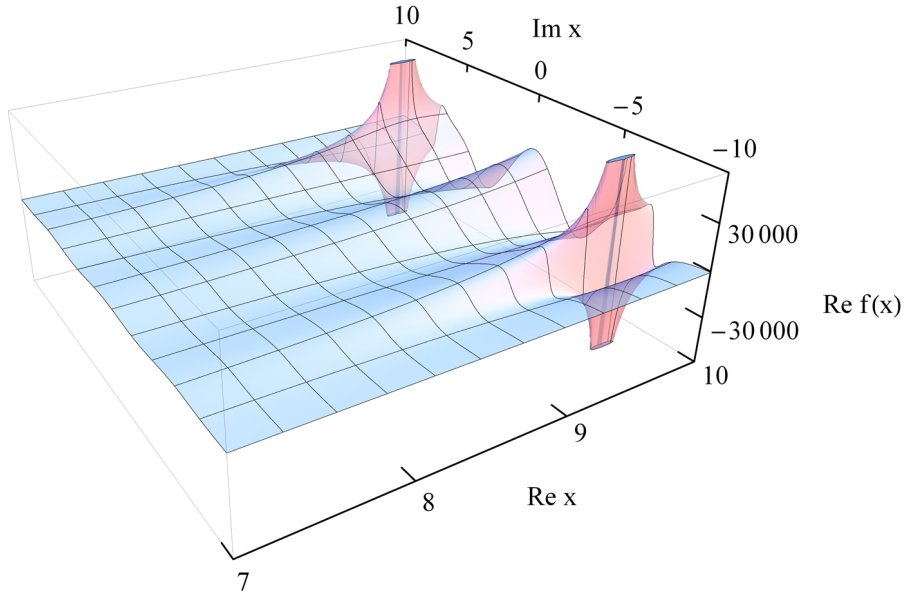

Model for a spectral function (I)

We use

$$\rho(\omega^2) = -\frac{1}{\pi}\mathrm{Im}\left(\frac{1}{\omega^2 - M^2 - \Pi(\omega^2)}\right)$$

with the self energy

$$\Pi(\omega^2) = S_1 \log(T_1^2 - \omega^2) + S_2 \log(T_2^2 - \omega^2)$$

and the parameters
$M = 50$ MeV,
$S_1 = 2000$ MeV^2,
$T_1 = 0$ MeV,
$S_2 = 3000$ MeV^2,
$T_2 = 300$ MeV,
$\omega \to \omega + i\varepsilon$ with $\varepsilon \to 0$

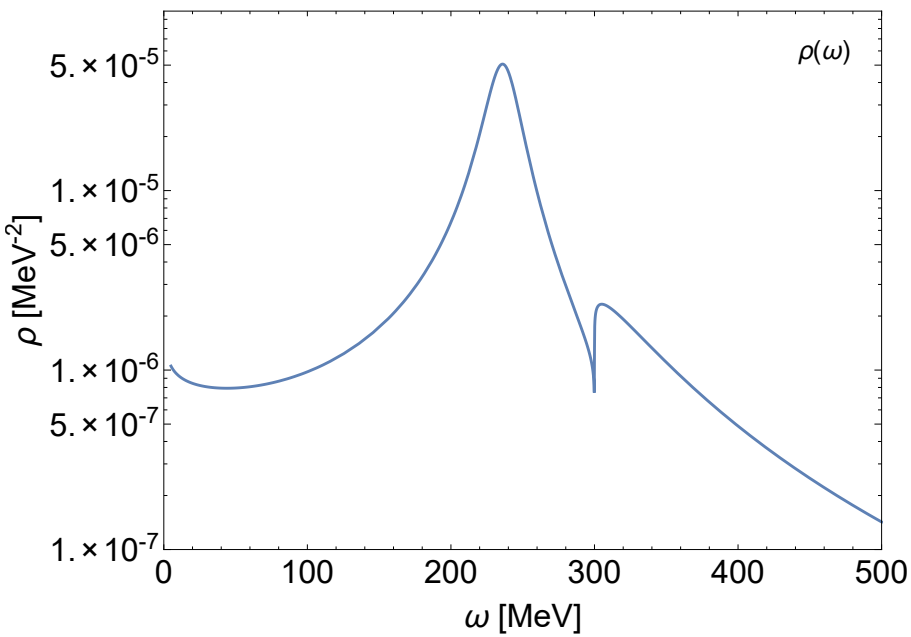

Model for a spectral function (II)

The decay thresholds at $T_1 = 0$ MeV and $T_2 = 300$ MeV represent branch points on the real axis.

Input 1 and 2 can be used to study the regime $T_1 < \omega < T_2$, Input 3 for $\omega > T_2$.

$N \approx 50$ input points were used for each regime.

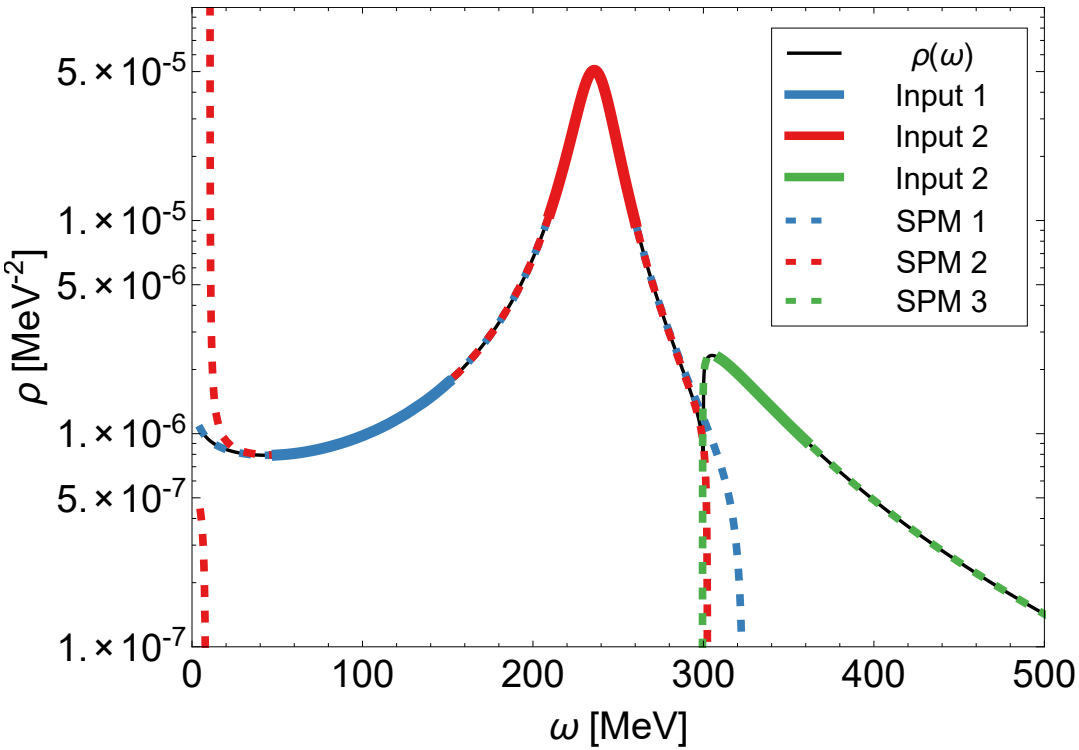

[R.-A. T., I. Haritan, J. Wambach and N. Moiseyev, arXiv:1610.03252]

Model for a spectral function (III)

The complex conjugate poles can be located by using SPM1 or SPM2:
$\omega_P \approx (236.43 \pm i12.64)$ MeV

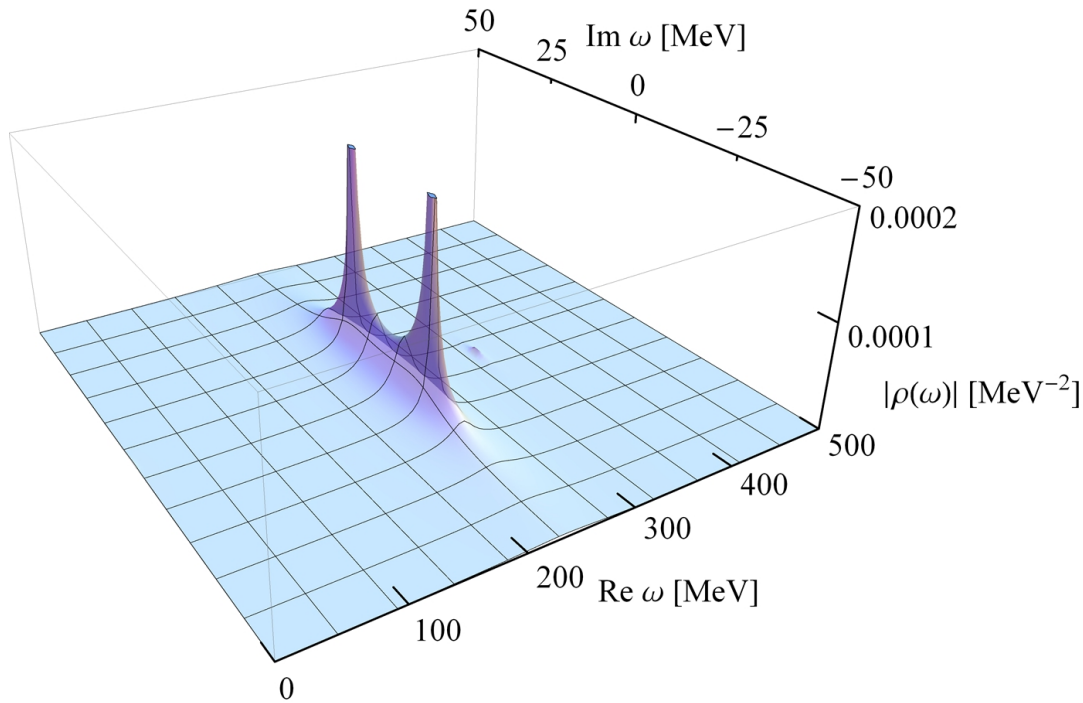

Model for overlapping resonances (I)

We use the Kühn-Santamaria (KS) parametrization for the form factor

$$F(s) = \sum_{i=1}^{3} \frac{M_i^2}{M_i^2 - s - i\Gamma_i \frac{M_i^2}{\sqrt{s}} \left(\frac{k(s)}{k(M_i^2)} \right)^3}$$

with

$$k(s) = \frac{\sqrt{s}}{2} \sqrt{1 - 4m_\pi^2/s}$$

and the parameters
$M_1 = 0.5$ GeV,
$\Gamma_1 = 0.2$ GeV,
$M_2 = 0.6$ GeV,
$\Gamma_2 = 0.1$ GeV,
$M_3 = 0.7$ GeV,
$\Gamma_3 = 0.15$ GeV,
$m_\pi = 0.137$ GeV

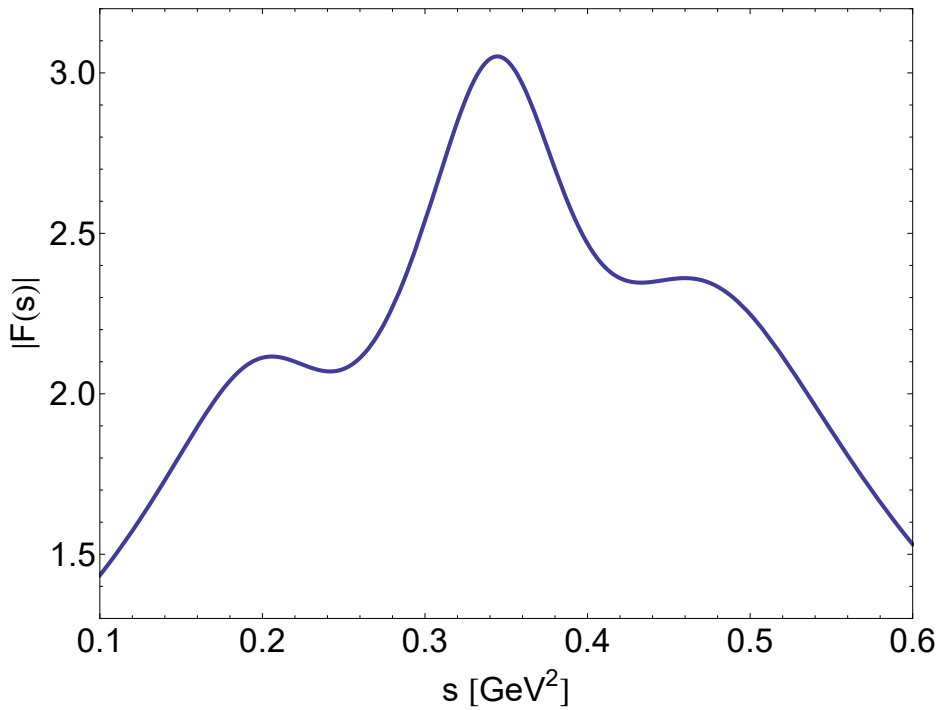

Model for overlapping resonances (II)

$N = 17$ input points were used.

All resonance poles can be reconstructed at the same time since they are in the same analytic regime.

Additional poles can appear in the reconstruction, but they can be easily identified as being unphysical by varying the number of input points or the input region.

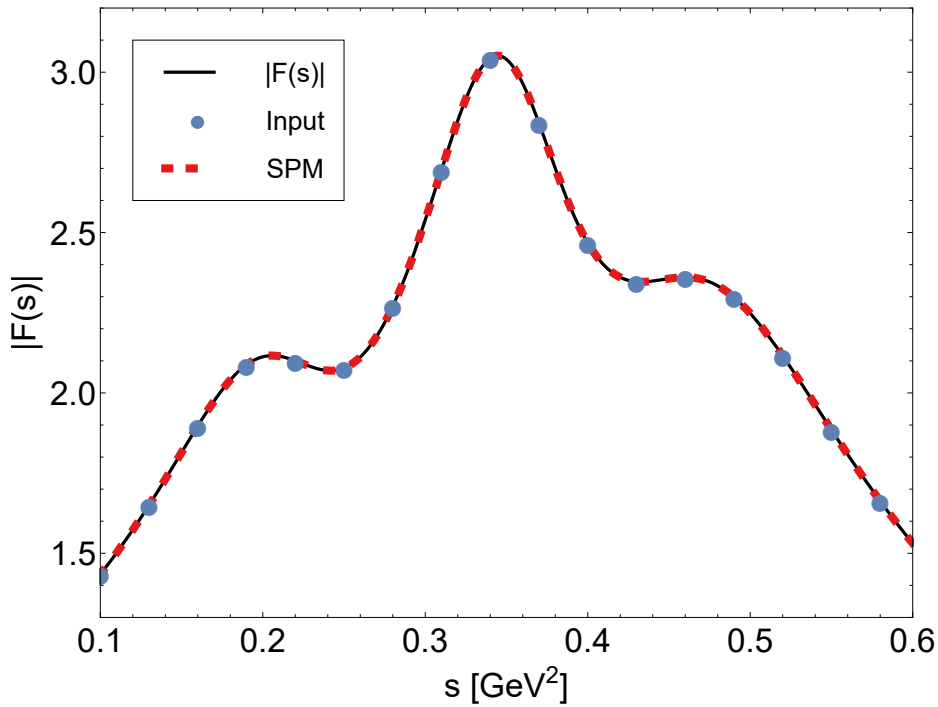

Model for overlapping resonances (III)

exact result, $F(s)$:

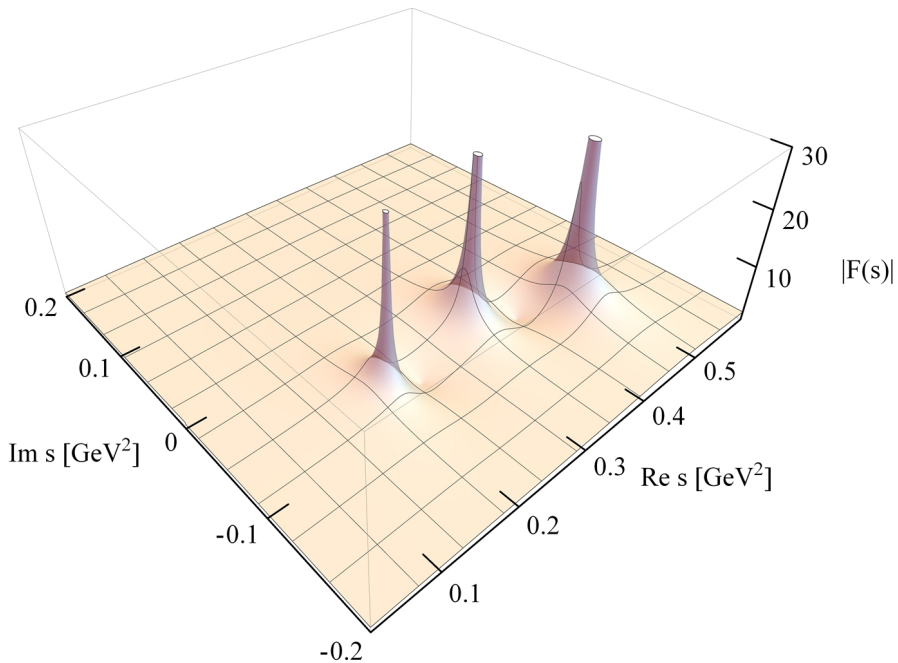

reconstruction, $C_N(s)$:

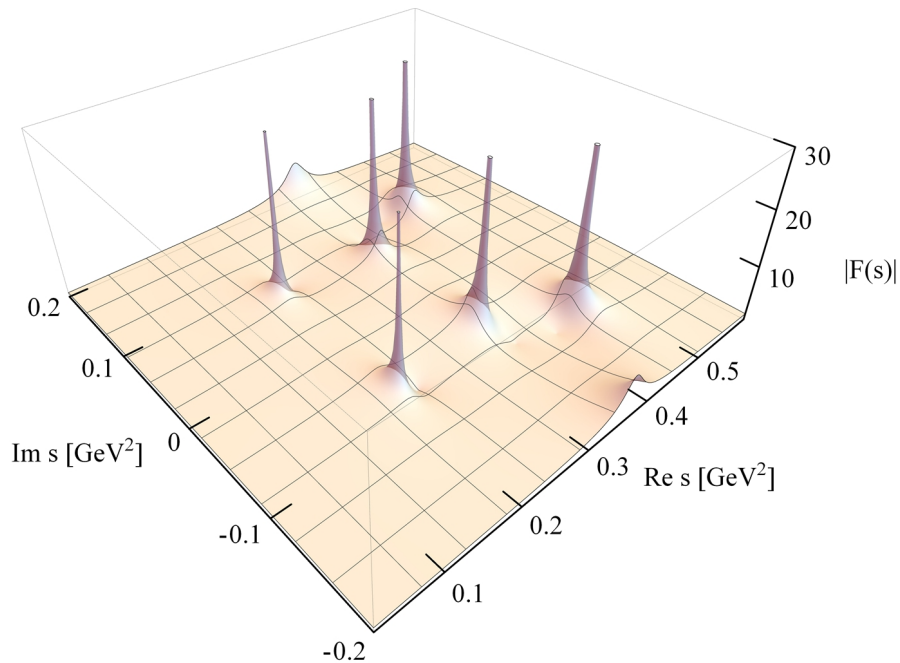

Complex pole of the charged $\rho(770)$ meson

We use the SPM method to analyze the ALEPH data on the squared modulus of the $\pi^-\pi^0$ vector form factor $|F_\pi(s)|^2$.

These data were obtained from τ-lepton decays and represent the cleanest determination of the $\rho(770)$-meson mass and width.

$\tau \to \pi^-\pi^0\nu_\tau$

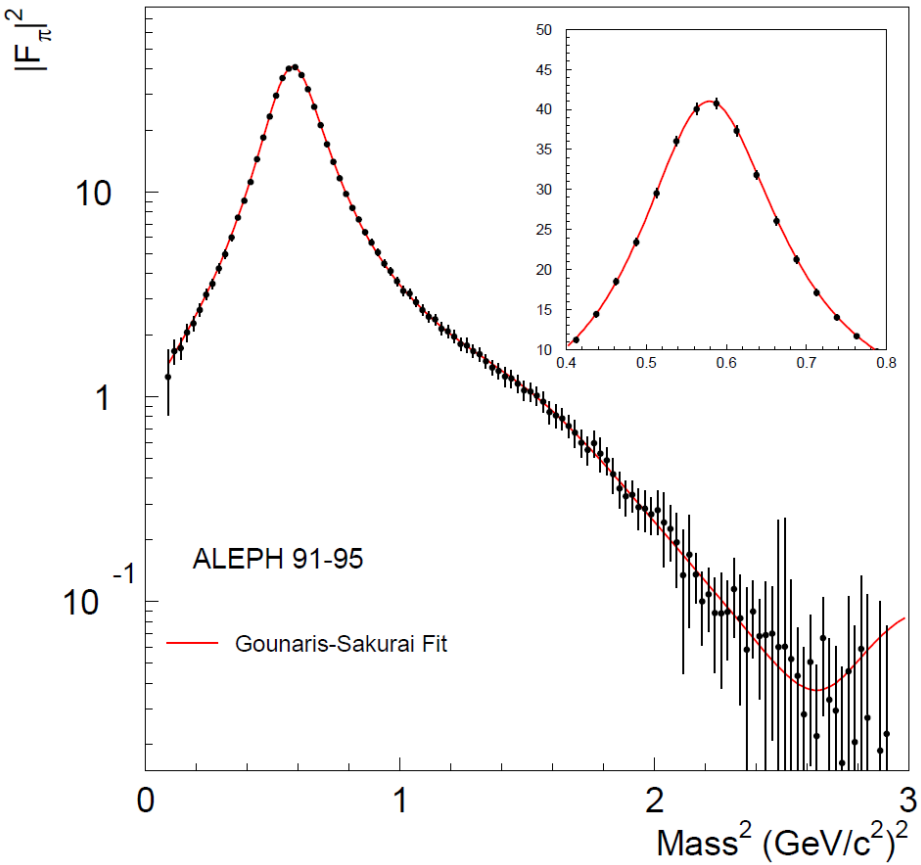

[ALEPH collaboration, Phys. Rept. 421, 191-284, 2005, arXiv:hep-ex/0506072]

Complex pole of the charged $\rho(770)$ meson

We use the SPM method to analyze the ALEPH data on the squared modulus of the $\pi^-\pi^0$ vector form factor $|F_\pi(s)|^2$.

We find the complex pole of the charged $\rho(770)$ meson to be at $\sqrt{s_\rho} = M_\rho - i\Gamma_\rho/2$ with

$$M_\rho = 761.8 \pm 1.9\,\text{MeV},$$
$$\Gamma_\rho = 139.8 \pm 3.6\,\text{MeV}.$$

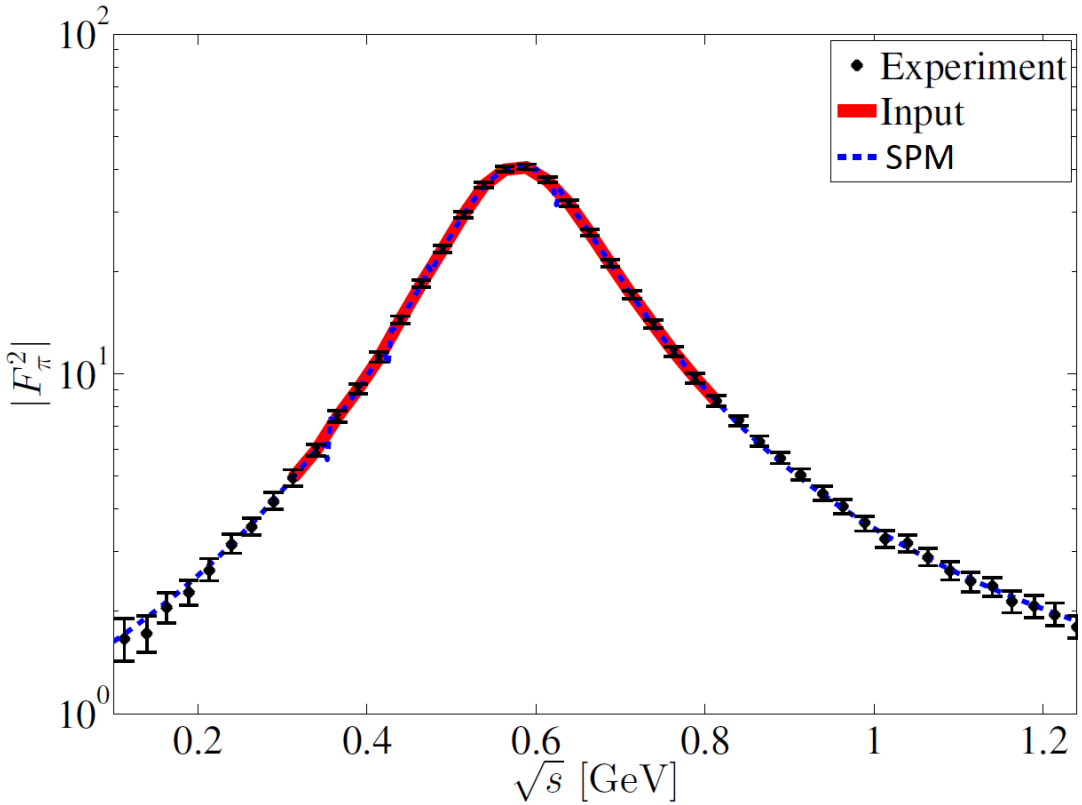

[R.-A. T., I. Haritan, J. Wambach and N. Moiseyev, arXiv:1610.03252]

Complex pole of the charged $\rho(770)$ meson

We use the SPM method to analyze the ALEPH data on the squared modulus of the $\pi^-\pi^0$ vector form factor $|F_\pi(s)|^2$.

We find the complex pole of the charged $\rho(770)$ meson to be at $\sqrt{s_\rho} = M_\rho - i\Gamma_\rho/2$ with

$$M_\rho = 761.8 \pm 1.9\,\text{MeV},$$
$$\Gamma_\rho = 139.8 \pm 3.6\,\text{MeV}.$$

M_ρ (MeV)	Γ_ρ (MeV)	source
762.5 ± 2	142 ± 7	[12]
758.3 ± 5.4	145.1 ± 6.3	[13]
$764.1 \pm 2.7^{+4.0}_{-2.5}$	$148.2 \pm 1.9^{+1.7}_{-5.0}$	[14]
754 ± 18	148 ± 20	[15]
763.0 ± 0.2	139.0 ± 0.5	[16]
760 ± 2	147 ± 6	[17]
761 ± 1	139 ± 2	[18]
763.7 ± 1.2	144 ± 3	[19]
761.8 ± 1.9	139.8 ± 3.6	this work

Table 1: Collection of pole parameter predictions for the $\rho(770)$ meson.

[R.-A. T., I. Haritan, J. Wambach and N. Moiseyev, arXiv:1610.03252]

Complex pole of the $f_0(500)$ or σ meson

Locating the resonance pole is particularly difficult for the $f_0(500)$ or σ meson due to its large decay width and the strong overlap with the background and higher resonances.

Plot: S0 wave phase shift for $\pi\pi$-scattering experimental data together with the UFD and CFD parameterizations.

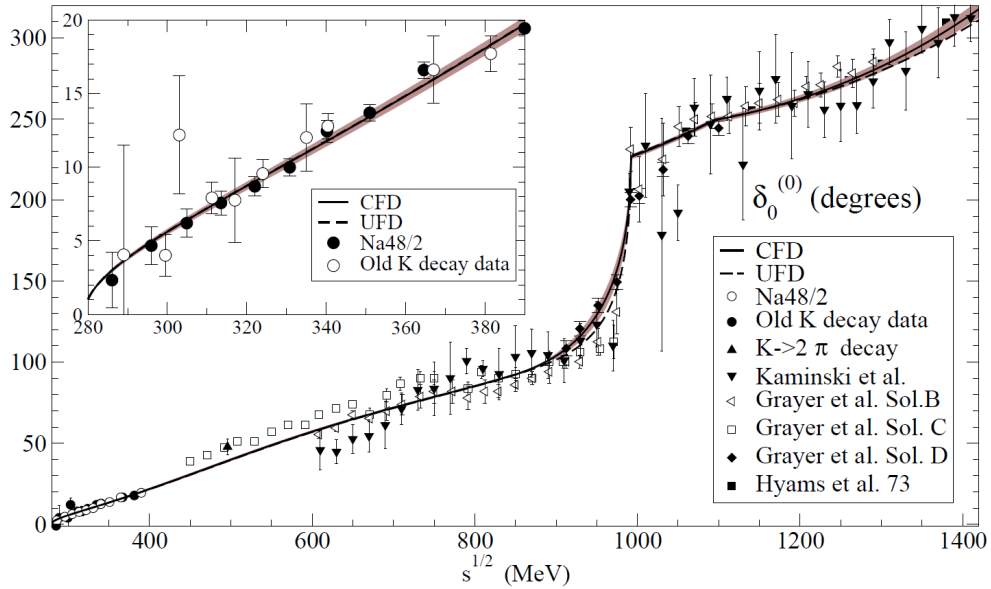

[R. Garcia-Martin, R. Kaminski, J. Pelaez, J. Ruiz de Elvira, and F. Yndurain, Phys.Rev. D83, 074004 (2011), arXiv:1102.2183 [hep-ph]]

Complex pole of the $f_0(500)$ or σ meson

We apply the SPM method to the real part of the S0 partial wave amplitude $t_0^0(s)$ as obtained from the Constrained Fit to Data (CFD) parametrization of the $\delta_0^{(0)}(s)$ phase shift,

$$t_0^0(s) = \frac{\eta_0^0(s)e^{2i\delta_0^0(s)} - 1}{2i\rho_\pi(s)}$$

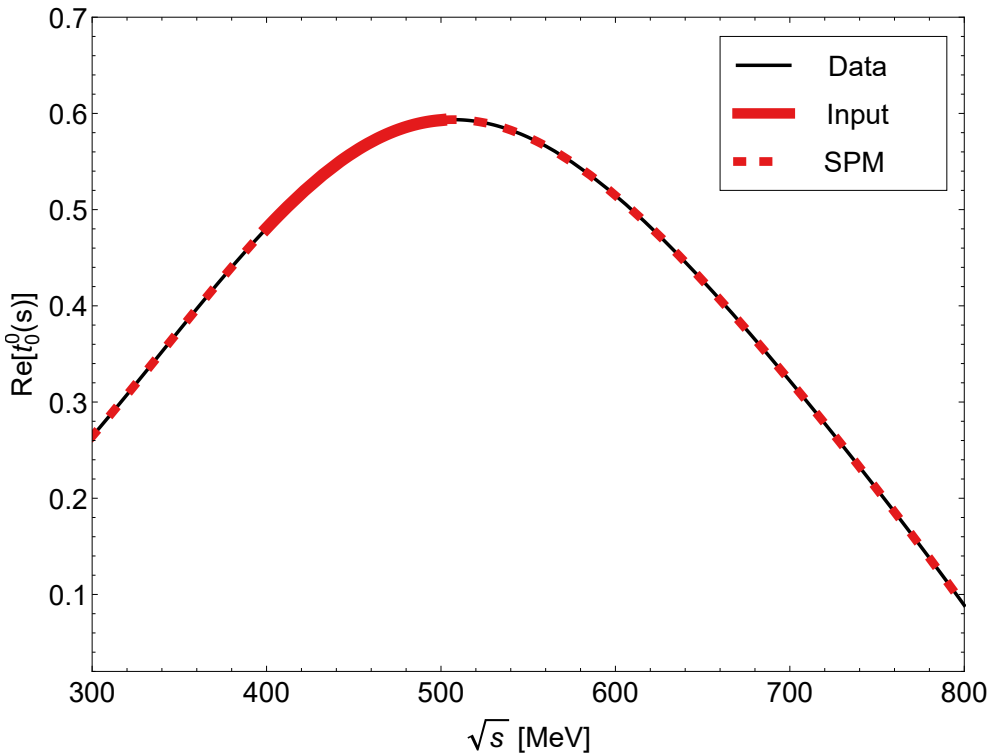

[R.-A. T., I. Haritan, J. Wambach and N. Moiseyev, arXiv:1610.03252]

We find the complex pole at $\sqrt{s_\sigma} = 450.1 \pm 11.2 - i(299.2 \pm 12.2)\,\text{MeV}$

Complex pole of the $f_0(500)$ or σ meson

$\sqrt{s_\sigma}$ (MeV)	source
$470 \pm 30 - i(295 \pm 20)$	[24]
$470 \pm 50 - i(285 \pm 25)$	[16]
$441^{+16}_{-8} - i(272^{+9}_{-12.5})$	[25]
$457^{+14}_{-13} - i(279^{+11}_{-7})$	[26]
$442^{+5}_{-8} - i(274^{+6}_{-5})$	[27]
$453 \pm 15 - i(297 \pm 15)$	[28]
$449^{+22}_{-16} - i(275 \pm 12)$	[20]
$450.1 \pm 11.2 - i(299.2 \pm 12.2)$	this work

Table 3: Collection of pole parameter predictions for the $f_0(500)$ or σ meson.

[R.-A. T., I. Haritan, J. Wambach and N. Moiseyev,

arXiv:1610.03252]

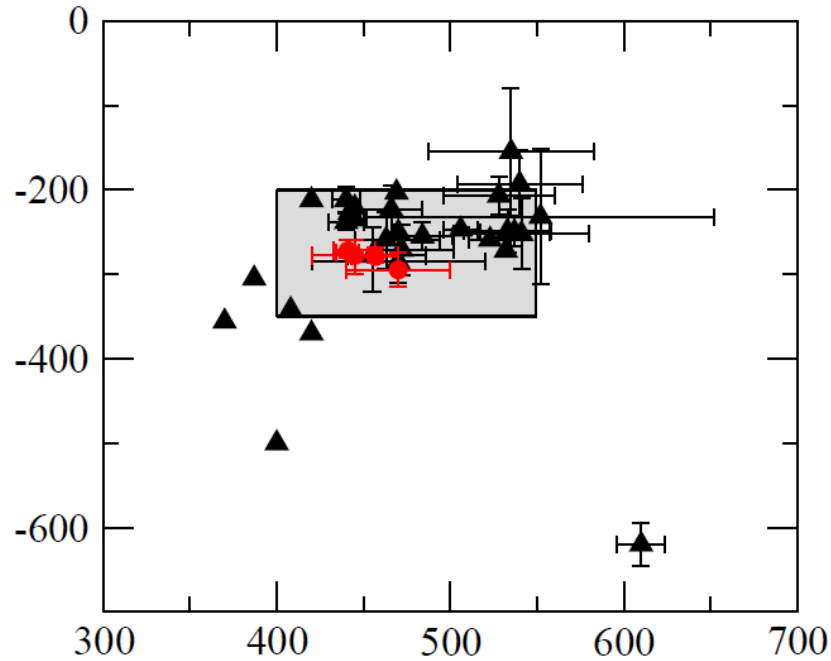

Figure 1: Location of the $f_0(500)$ (or σ) poles in the complex energy plane. Circles denote the recent analyses based on Roy(-like) dispersion relations [8–11], while all other analyses are denoted by triangles. The corresponding references are given in the listing.

[K.A. Olive et al. (Particle Data Group), Chin. Phys. C38, 090001 (2014) (URL: http://pdg.lbl.gov)]

Analytic Continuation - Free Particle

We want to reconstruct the spectral function of a free particle:

$$\rho(\omega) = \text{sgn}(\omega)\delta(\omega^2 - m^2)$$

The free propagator is given by

$$D^E(p_0) = \frac{1}{p_0^2 + m^2}$$

with $p_0 = 2n\pi T$,
$m = 200$ MeV, and
$T = 1/\beta = 10$ MeV.

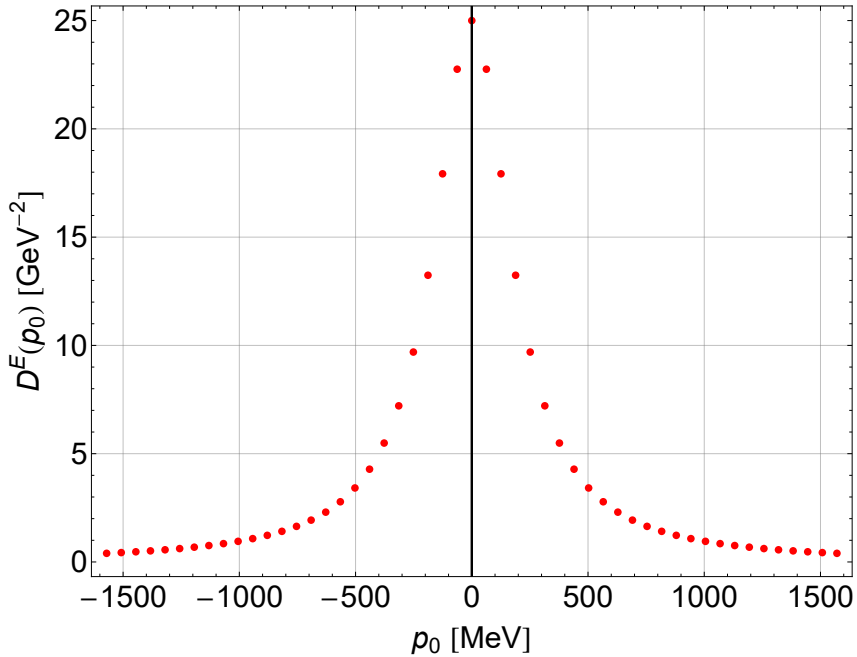

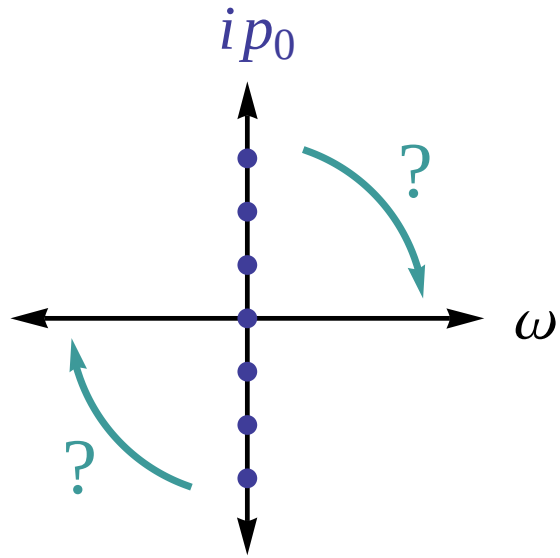

Analytic Continuation - Free Particle

We choose 51 input points from $D^E(p_0)$ and apply the SPM to obtain $D^R(\omega)$ and the spectral function,

$$\rho(\omega) = -\frac{1}{\pi}\mathrm{Im}D^R(\omega)$$

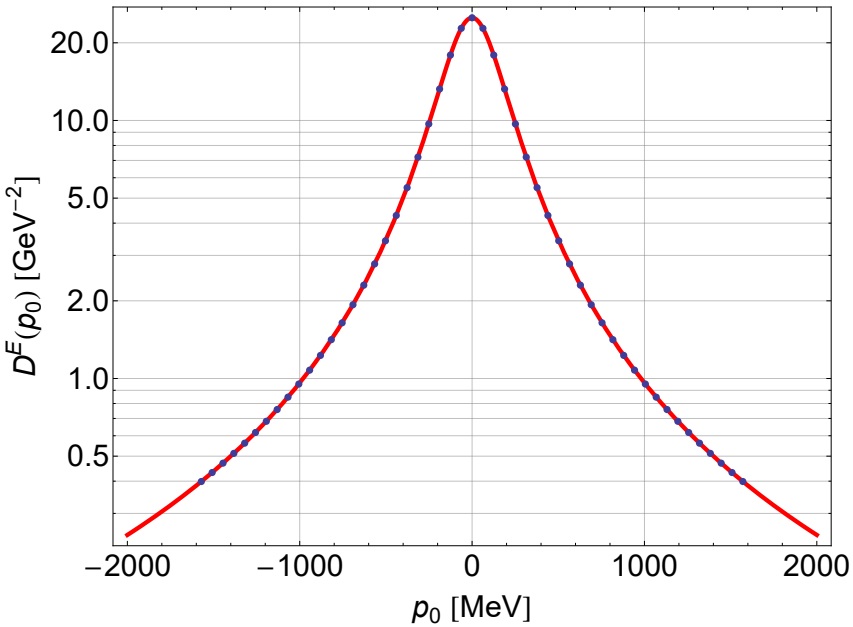

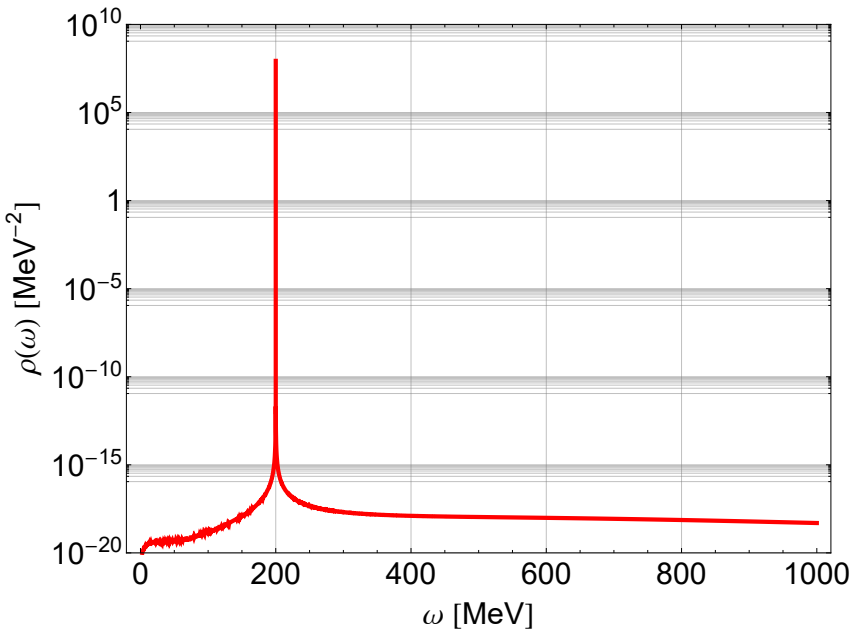

Analytic Continuation - Model for Spectral Function

We now study the following spectral function,

$$\rho(\omega) = -\frac{1}{\pi}\mathrm{Im}\left(\frac{1}{(\omega+i\epsilon)^2 - M^2 - \Pi(\omega)}\right)$$

with

$$\begin{aligned}\Pi(\omega) =& S_1(\ln(T_1^2 - (\omega+i\epsilon)^2)) \\ &+ S_2(\ln(T_2^2 - (\omega+i\epsilon)^2))\end{aligned}$$

We choose $M = 50$ MeV, $\epsilon = 0.1$ MeV, $T = 1/\beta = 10$ MeV, $S_1 = 2000$, $S_2 = 300$, $T_1 = 0$ and $T_2 = 3000$.

The propagator is obtained by

$$D^E(p_0) = \int_{-\infty}^{\infty} d\omega \frac{\rho(\omega)}{\omega + ip_0}$$

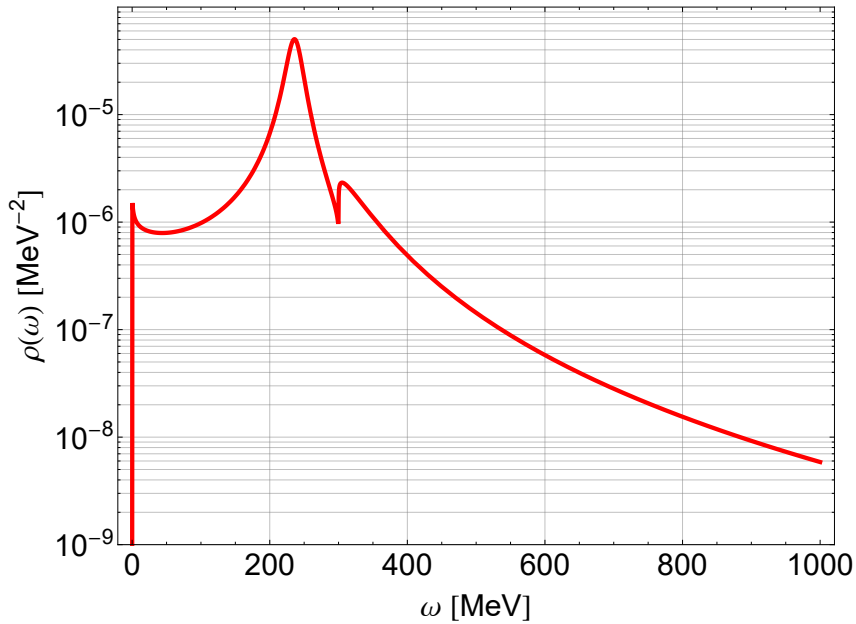

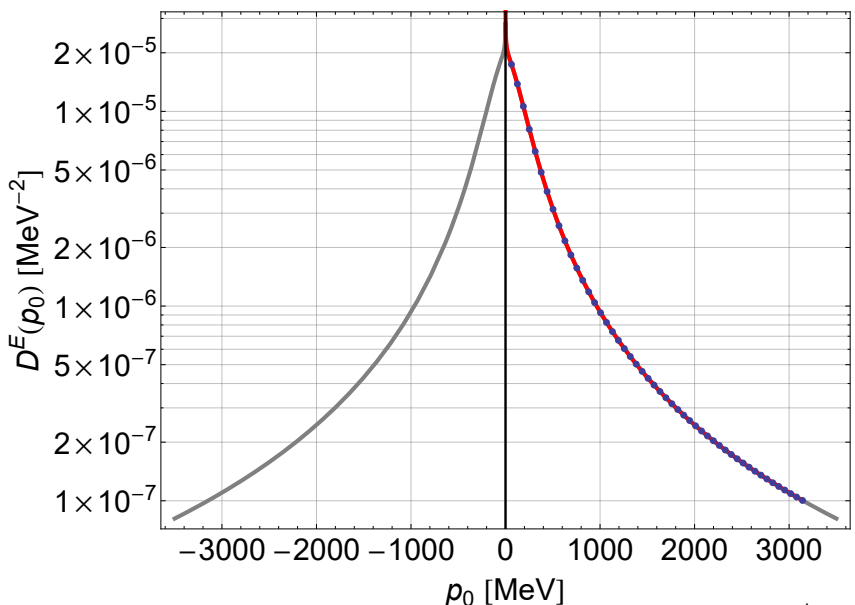

Analytic Continuation - Model for Spectral Function

We choose 51 input points from $D^E(p_0)$ and apply the SPM to obtain $D^R(\omega)$ and the spectral function,

$$\rho(\omega) = -\frac{1}{\pi}\mathrm{Im}D^R(\omega)$$

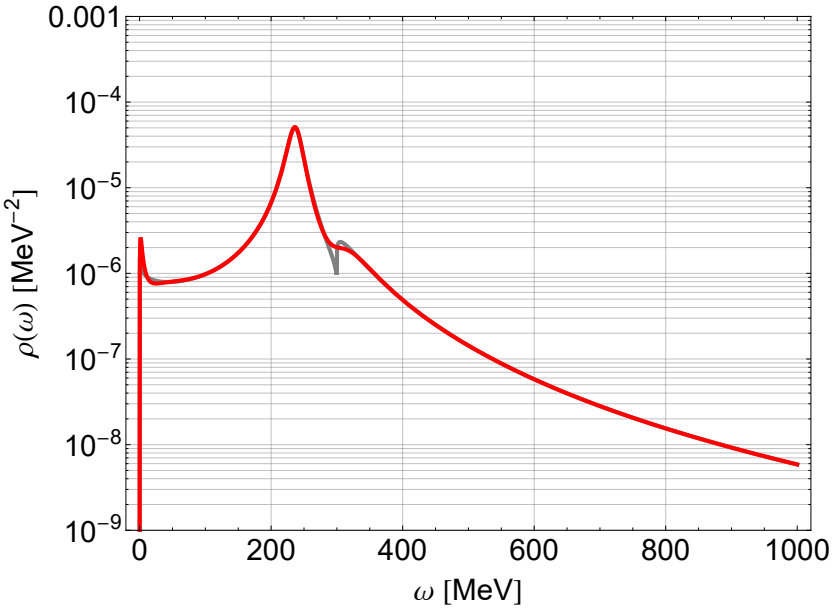

We only get one pole in the complex plane close to the peak of the spectral function:

$(x_P, y_P) = (236.93, -12.47)$ MeV

which is close to the exact location at

$(x_P, y_P) = (236.43, -12.64)$ MeV.

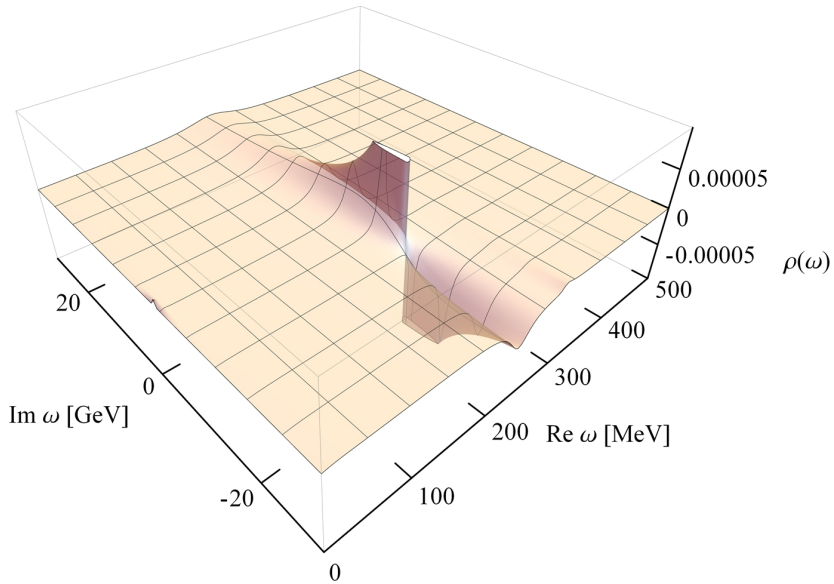

Analytic continuation of Euclidean FRG data

- We start from data on the Euclidean 2-point function $\Gamma^{(2),E}(ip_0)$ for the pion at $T = 2$ MeV which was obtained using the Functional Renormalization Group approach (FRG)

- The SPM method is used to obtain the analytic continuation $\Gamma^{(2),R}(\omega)$

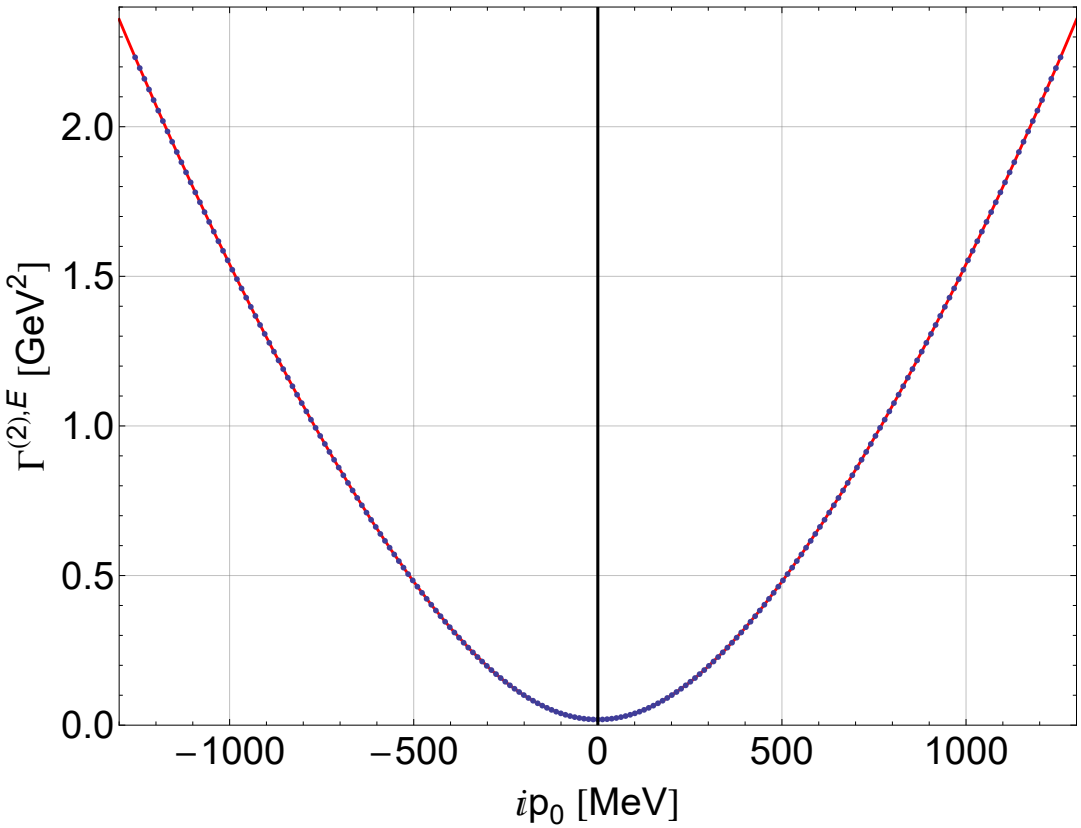

Analytic continuation of Euclidean FRG data

- the spectral function consists of a delta peak at $\omega \approx 100$ MeV and a continuum starting at $\omega \approx 600$ MeV

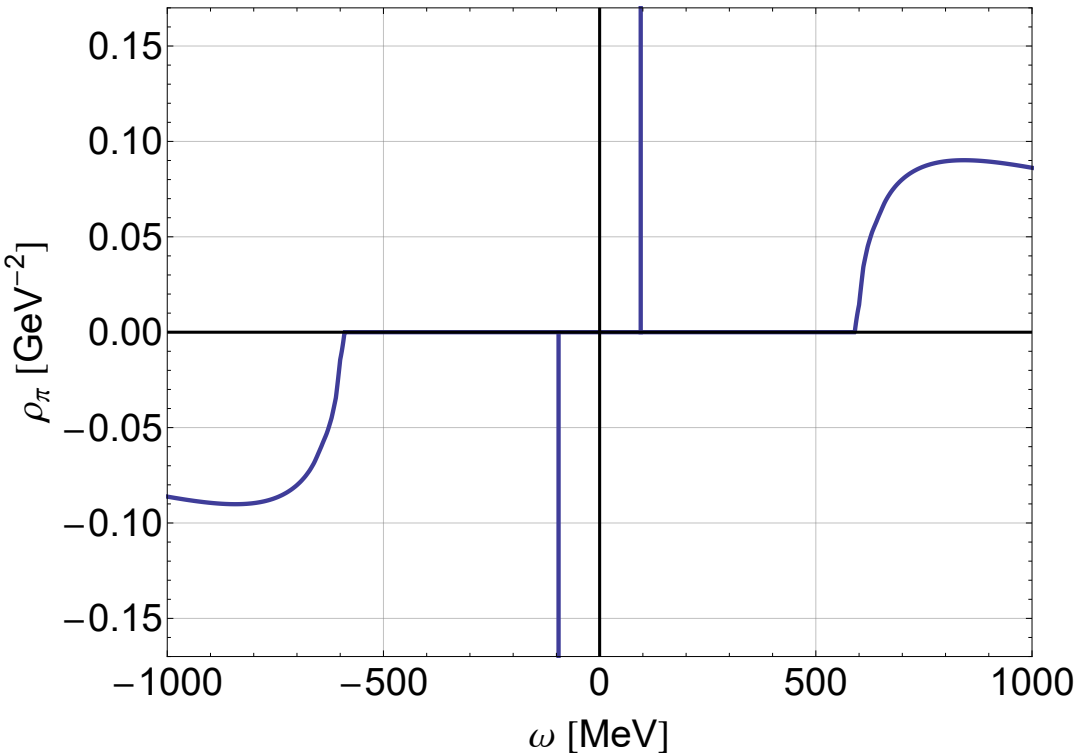

$$\rho(\omega) = -\frac{1}{\pi}\mathrm{Im}G^R(\omega) = \frac{1}{\pi}\frac{\mathrm{Im}\Gamma^{(2),R}(\omega)}{(\mathrm{Re}\Gamma^{(2),R}(\omega))^2 + (\mathrm{Im}\Gamma^{(2),R}(\omega))^2}$$

Analytic continuation of Euclidean FRG data

- $N = 65$ Euclidean input points between $p_0 = 0$ MeV and $p_0 = 2000$ MeV are used
- we obtain a good reconstruction of the spectral function even for energies beyond the branch point at $\omega = 600$ MeV

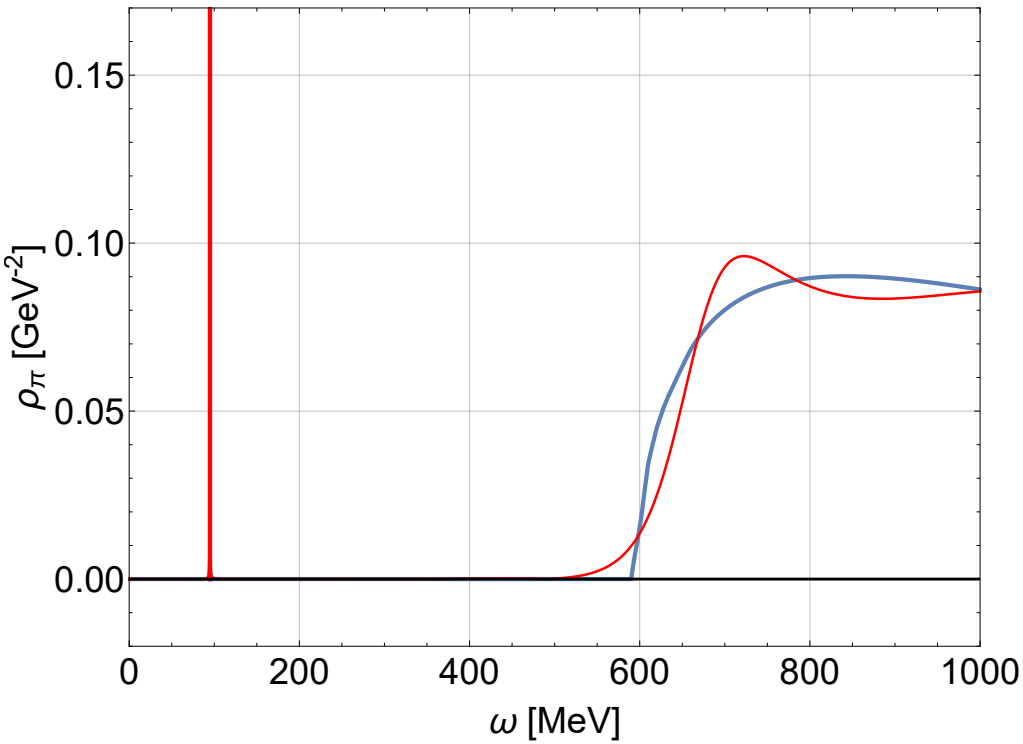

Analytic continuation of simulated DSE data

- data obtained from Dyson-Schwinger equations (DSE) is usually obtained for Euclidean momenta $p^2 > 0$
- We want to reconstruct the function

$$f(p^2) = \frac{1}{p^2 + 5 + \log(p^2 + 20)}$$

- we select 45 non-equidistant points within $p^2 \in [0.001, 50]$ GeV^2

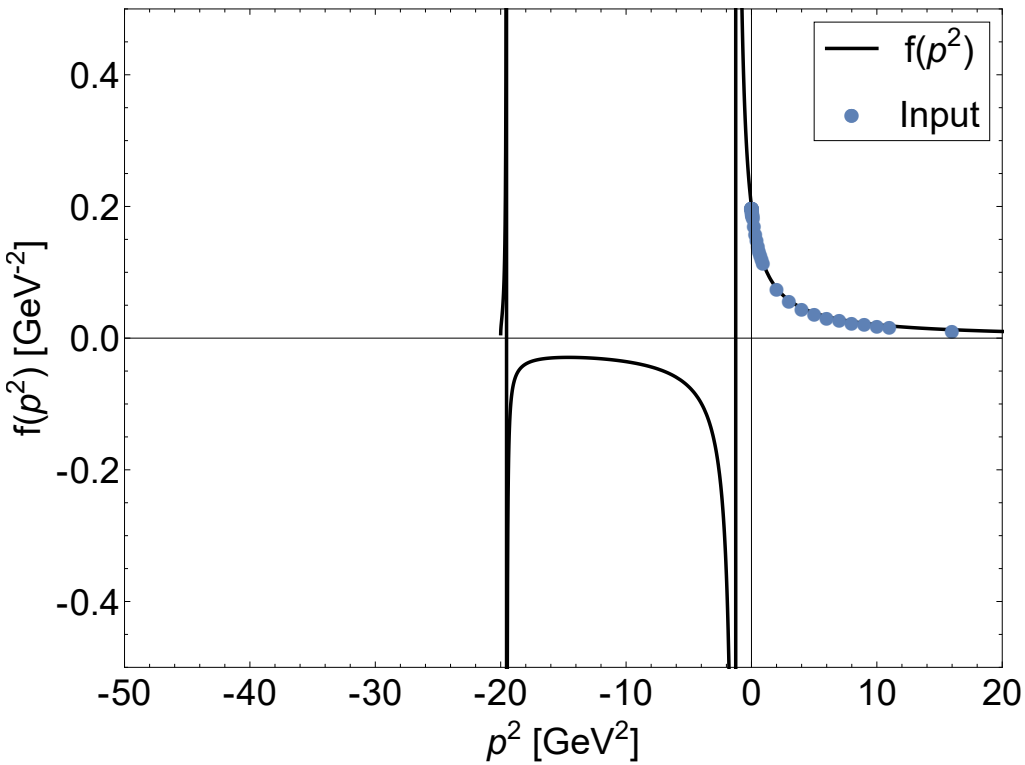

Analytic continuation of simulated DSE data

- We want to reconstruct the function

$$f(p^2) = \frac{1}{p^2 + 5 + \log(p^2 + 20)}$$

- we select 45 non-equidistant points within $p^2 \in [0.001, 50]$ GeV^2

- the branch cut is represented by the SPM method as a series of poles
- the location of these poles depend on the chosen input points

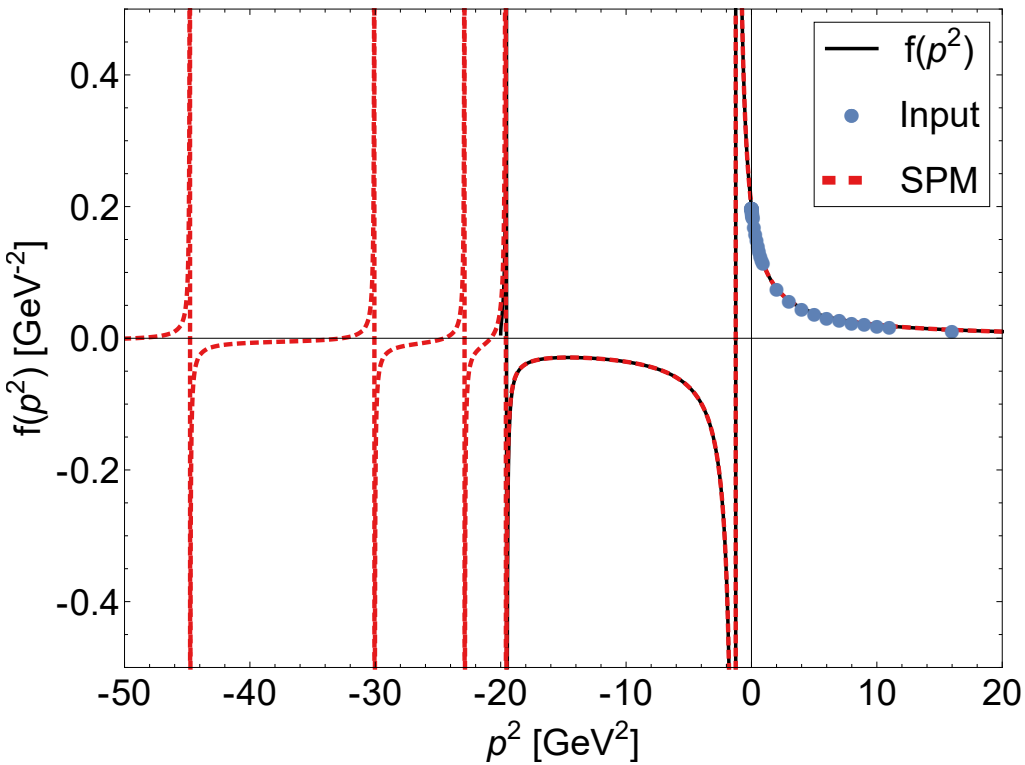

Analytic continuation of simulated DSE data

- We want to reconstruct the function

$$f(p^2) = \frac{1}{p^2 + 5 + \log(p^2 + 20)}$$

- now we take the same input points as before but rescale the x values: $p_0^2 \to p_0$ and then evaluate at $f(ip_0)$

- the branch cut is now clearly visible in the imaginary part of the SPM reconstruction

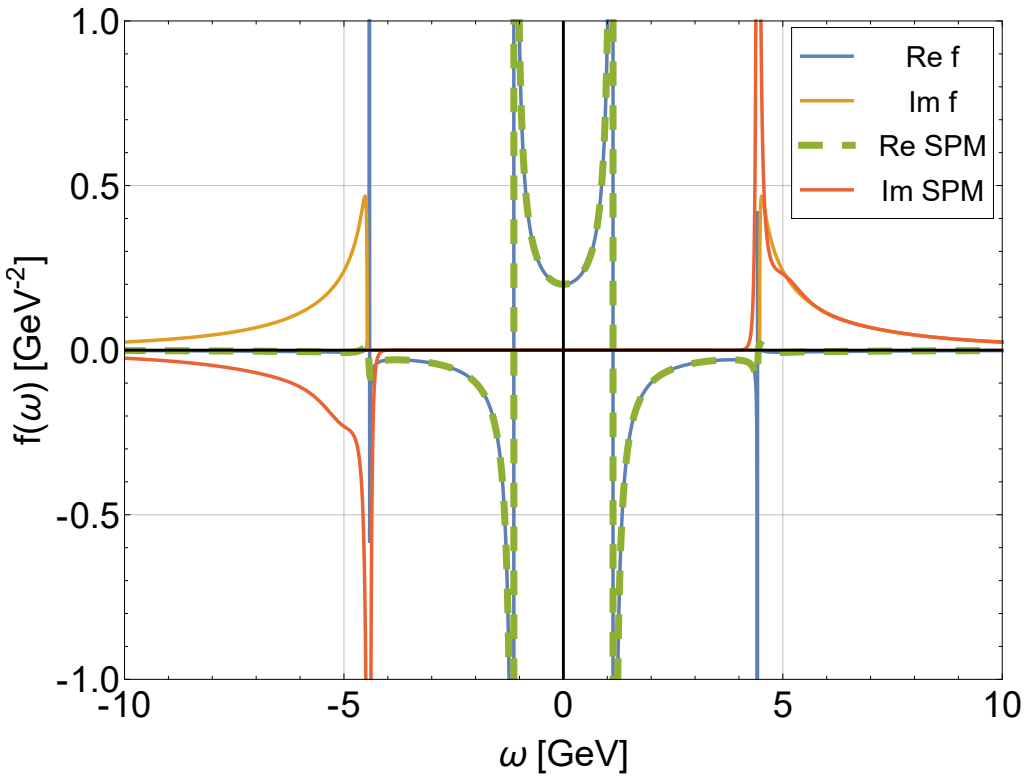

Direct comparison of MEM, BGM and SPM - preliminary

- We now study the following Breit-Wigner type model for a spectral function,

$$\rho(\omega) = \frac{1}{\pi} \frac{2\omega\epsilon}{(\omega^2 - \epsilon^2 - M^2)^2 + 4\omega^2\epsilon^2}$$

- we choose $M = 300$ MeV, $\epsilon = 100$ MeV and $T = 2$ MeV
- we will use data on the Euclidean correlator $G^E(\tau)$ for the Maximum Entropy Method (MEM), the Backus-Gilbert method (BGM) and the Schlessinger Point Method (SPM)

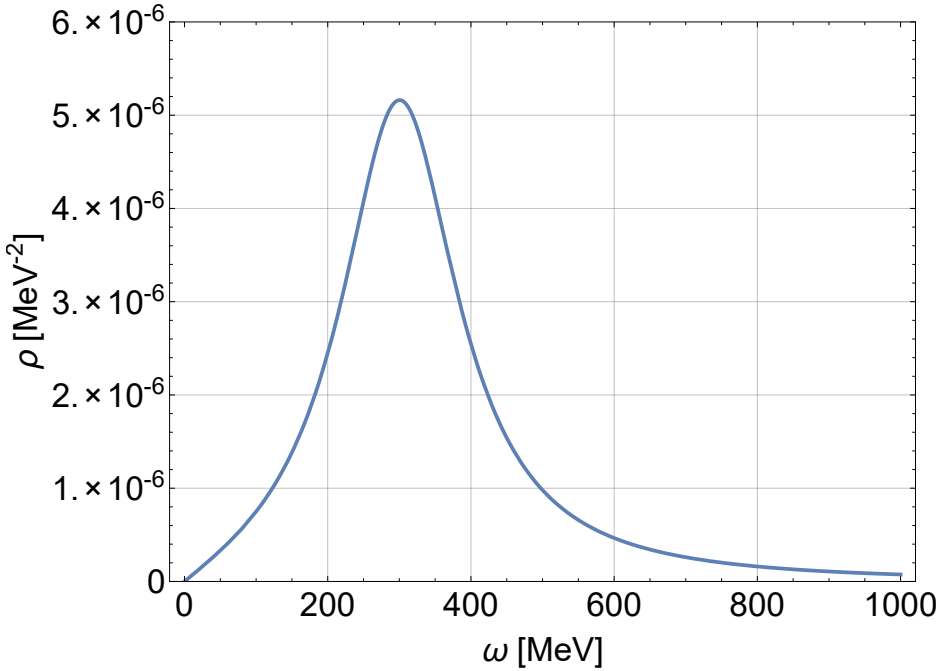

[R.-A. T., P. Gubler, M. Ulybyshev and L. von Smekal, in preparation]

Direct comparison of MEM, BGM and SPM - preliminary

- We now study the following Breit-Wigner type model for a spectral function,

$$\rho(\omega) = \frac{1}{\pi} \frac{2\omega\epsilon}{(\omega^2 - \epsilon^2 - M^2)^2 + 4\omega^2\epsilon^2}$$

- we choose $M = 300$ MeV, $\epsilon = 100$ MeV and $T = 2$ MeV
- we will use data on the Euclidean correlator $G^E(\tau)$ for the Maximum Entropy Method (MEM), the Backus-Gilbert method (BGM) and the Schlessinger Point Method (SPM)

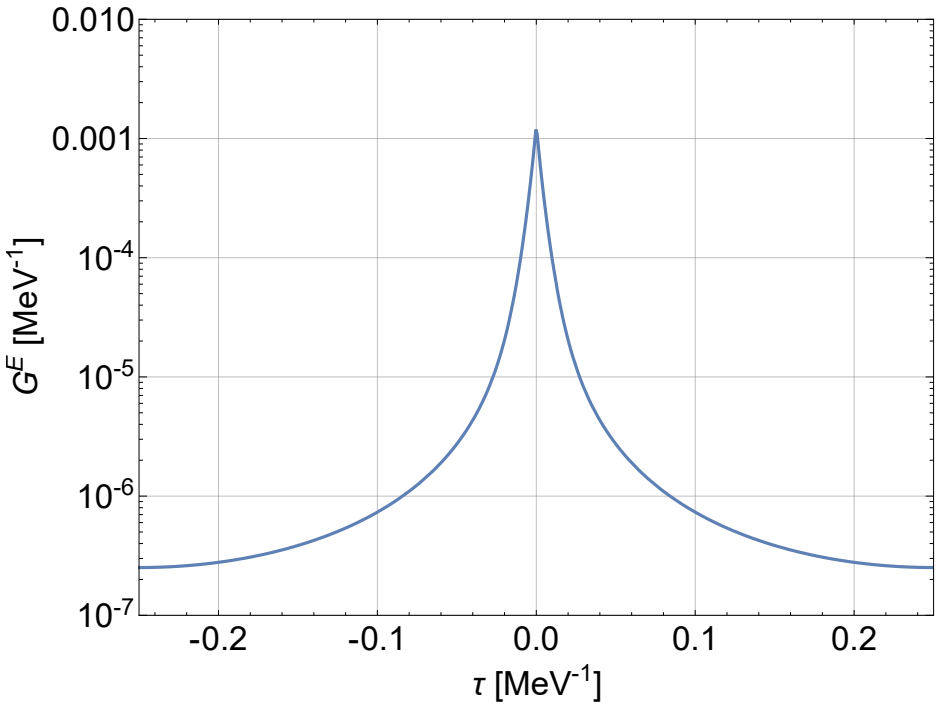

[R.-A. T., P. Gubler, M. Ulybyshev and L. von Smekal, in preparation]

Direct comparison of MEM, BGM and SPM - preliminary

- We now study the following Breit-Wigner type model for a spectral function,

$$\rho(\omega) = \frac{1}{\pi} \frac{2\omega\epsilon}{(\omega^2 - \epsilon^2 - M^2)^2 + 4\omega^2\epsilon^2}$$

- we choose $M = 300$ MeV, $\epsilon = 100$ MeV and $T = 2$ MeV
- we will use Euclidean input data for the Maximum Entropy Method (MEM), the Backus-Gilbert method (BGM) and the Schlessinger Point Method (SPM)

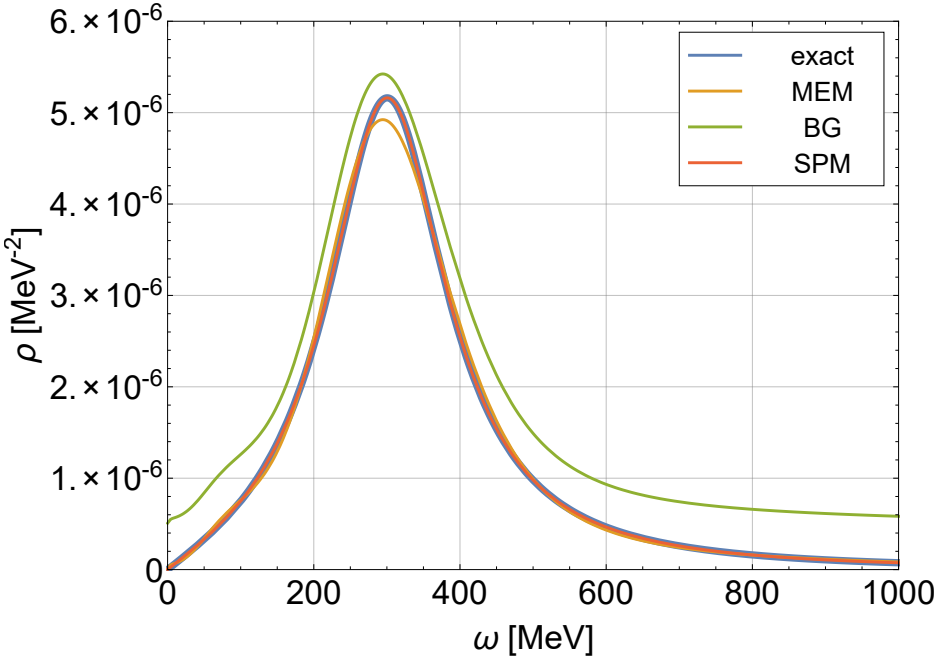

[R.-A. T., P. Gubler, M. Ulybyshev and L. von Smekal, in preparation]

SPM - dependence on N_τ and σ - preliminary

We add Gaussian noise of the form $f(x) = \frac{1}{\sqrt{2\pi}\sigma} e^{-\frac{(x-\mu)^2}{2\sigma^2}}$ to the data

$N_\tau = 64$:

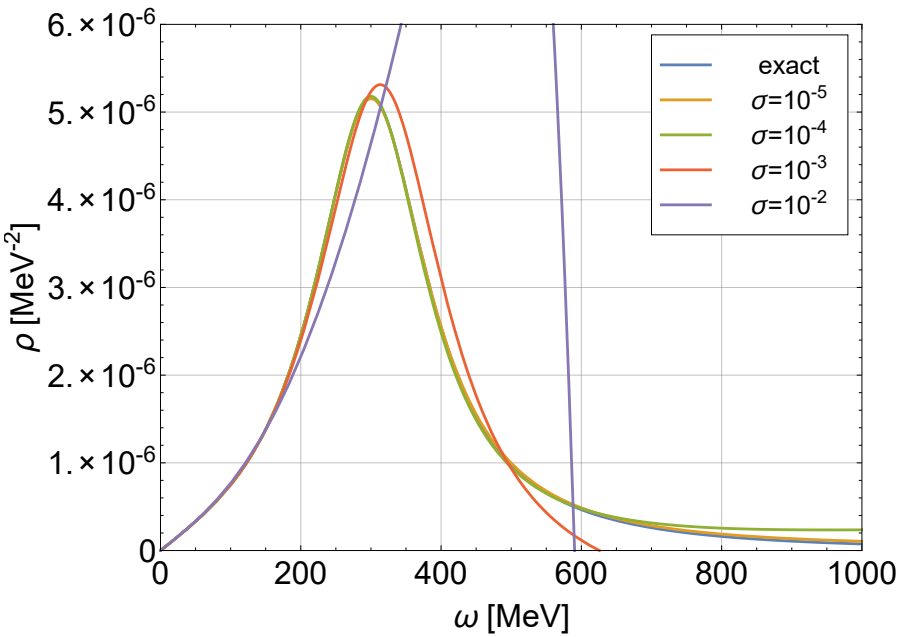

$\sigma = 10^{-3}$:

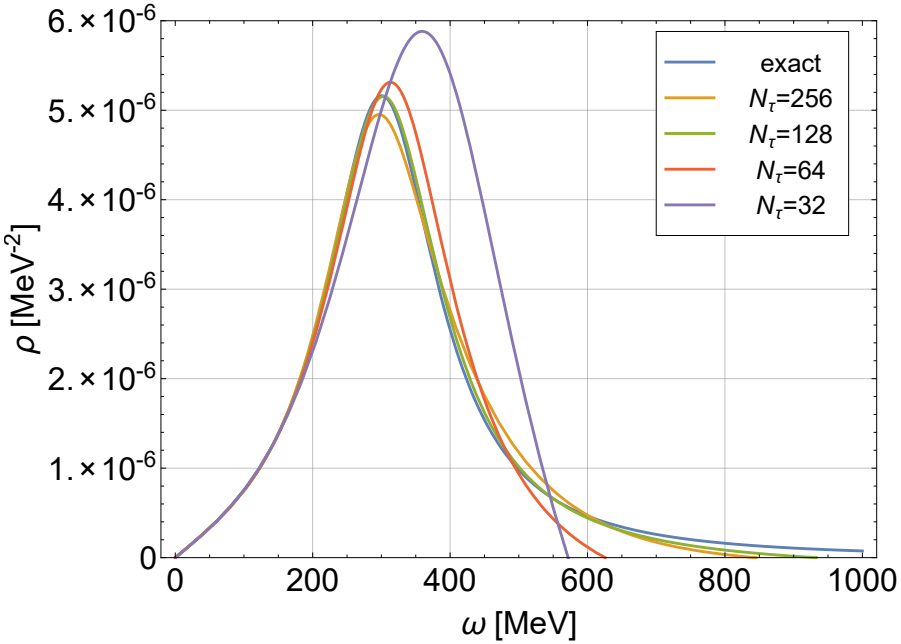

[R.-A. T., P. Gubler, M. Ulybyshev and L. von Smekal, in preparation]

MEM - dependence on N_τ and σ - preliminary

We add Gaussian noise of the form $f(x) = \frac{1}{\sqrt{2\pi}\sigma} e^{-\frac{(x-\mu)^2}{2\sigma^2}}$ to the data

$N_\tau = 64$:

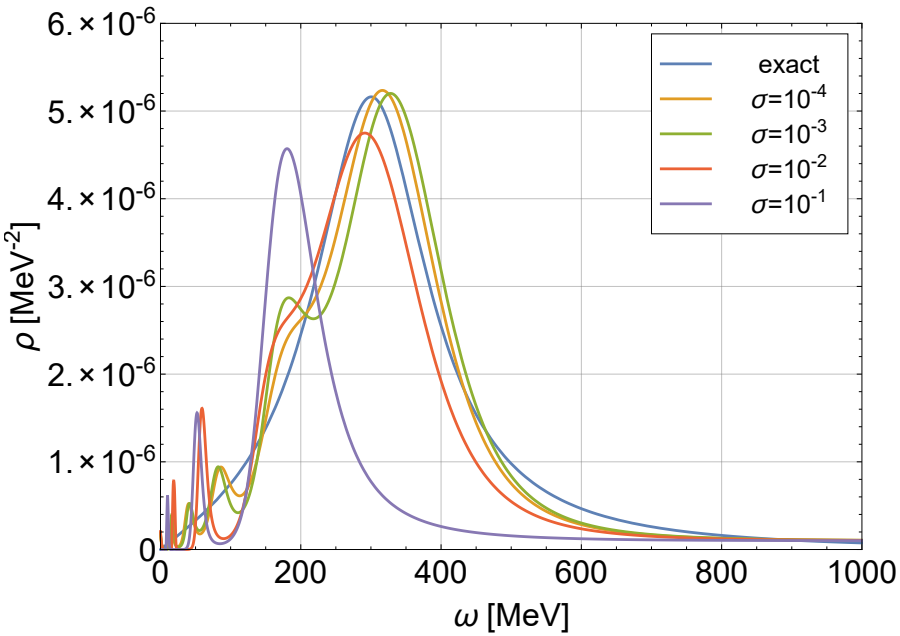

$\sigma = 10^{-3}$:

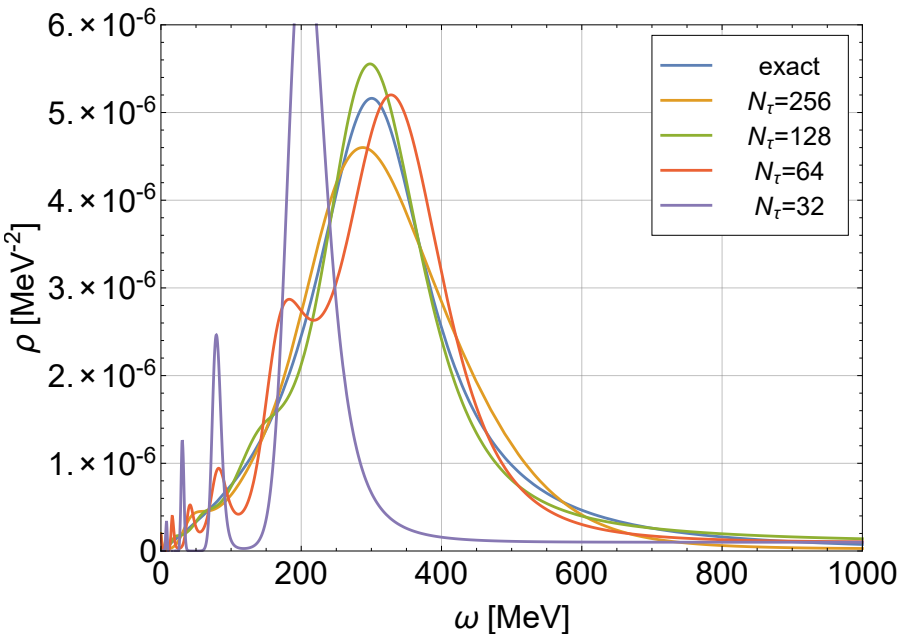

[R.-A. T., P. Gubler, M. Ulybyshev and L. von Smekal, in preparation]

BG - dependence on N_τ and σ - preliminary

We add Gaussian noise of the form $f(x) = \frac{1}{\sqrt{2\pi}\sigma} e^{-\frac{(x-\mu)^2}{2\sigma^2}}$ to the data

$N_\tau = 64$:

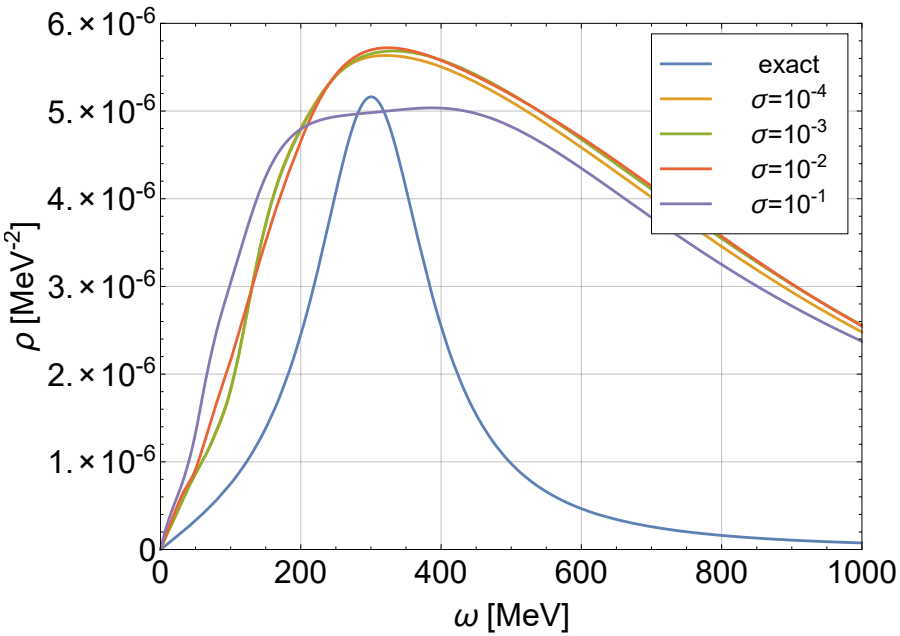

$\sigma = 10^{-3}$:

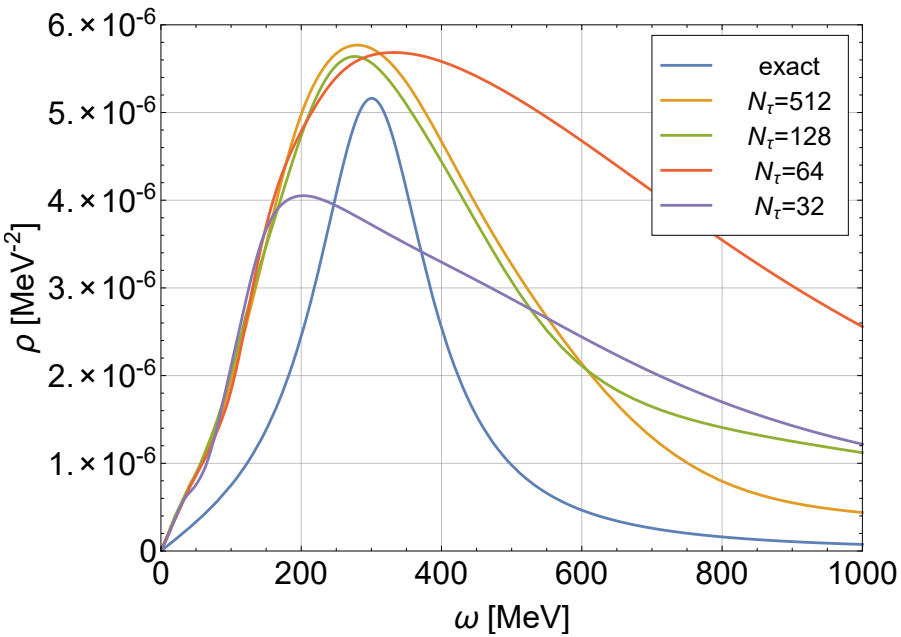

[R.-A. T., P. Gubler, M. Ulybyshev and L. von Smekal, in preparation]

Direct comparison of MEM, BGM and SPM - preliminary

- We add Gaussian noise of the form

$$f(x) = \frac{1}{\sqrt{2\pi}\sigma} e^{-\frac{(x-\mu)^2}{2\sigma^2}}$$

  to the data, with $\mu = y_i$ and different values for σ
- the regime of applicability is shown in dependence on the number of input points for $D(\tau)$ and the relative error of the data with parameter σ

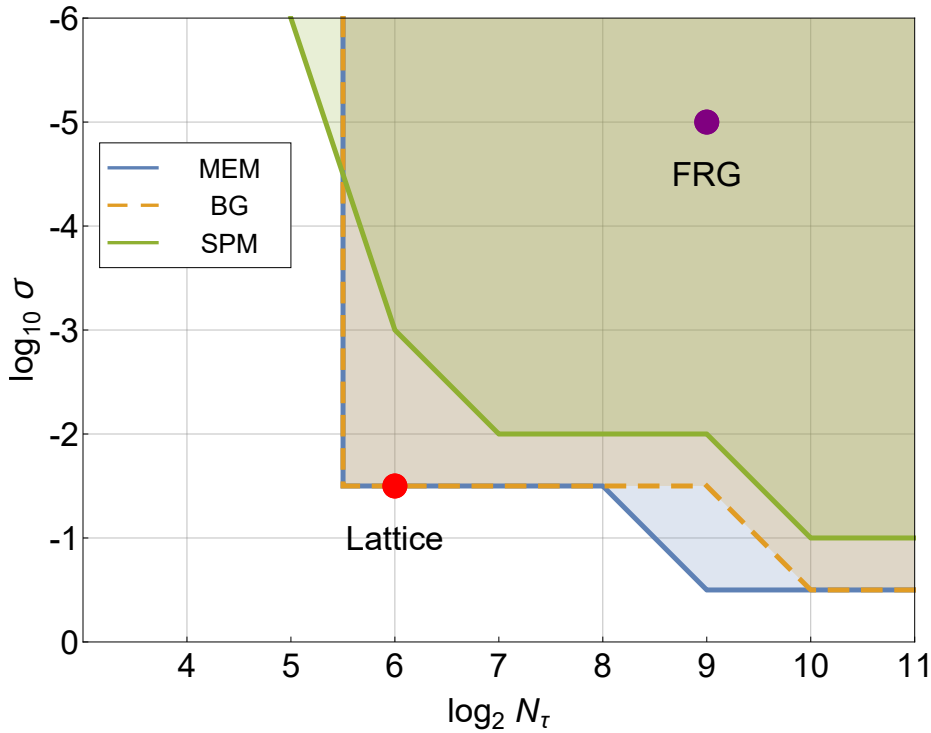

[R.-A. T., P. Gubler, M. Ulybyshev and L. von Smekal, in preparation]

Direct comparison of MEM, BGM and SPM - preliminary - FRG

- Comparison of the exact FRG spectral function for the pion at $T = 2$ MeV with the reconstructions obtained by using Euclidean data as input for the Maximum Entropy Method, the Backus-Gilbert method and the Schlessinger point method

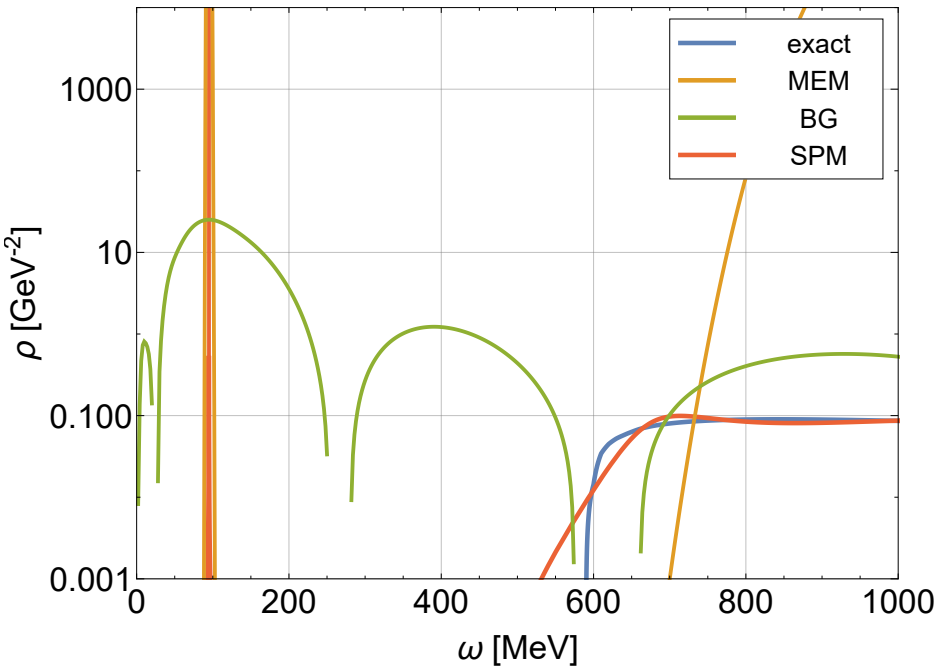

[R.-A. T., P. Gubler, M. Ulybyshev and L. von Smekal, in preparation]

Direct comparison of MEM, BGM and SPM - preliminary - Lattice data on the ρ meson

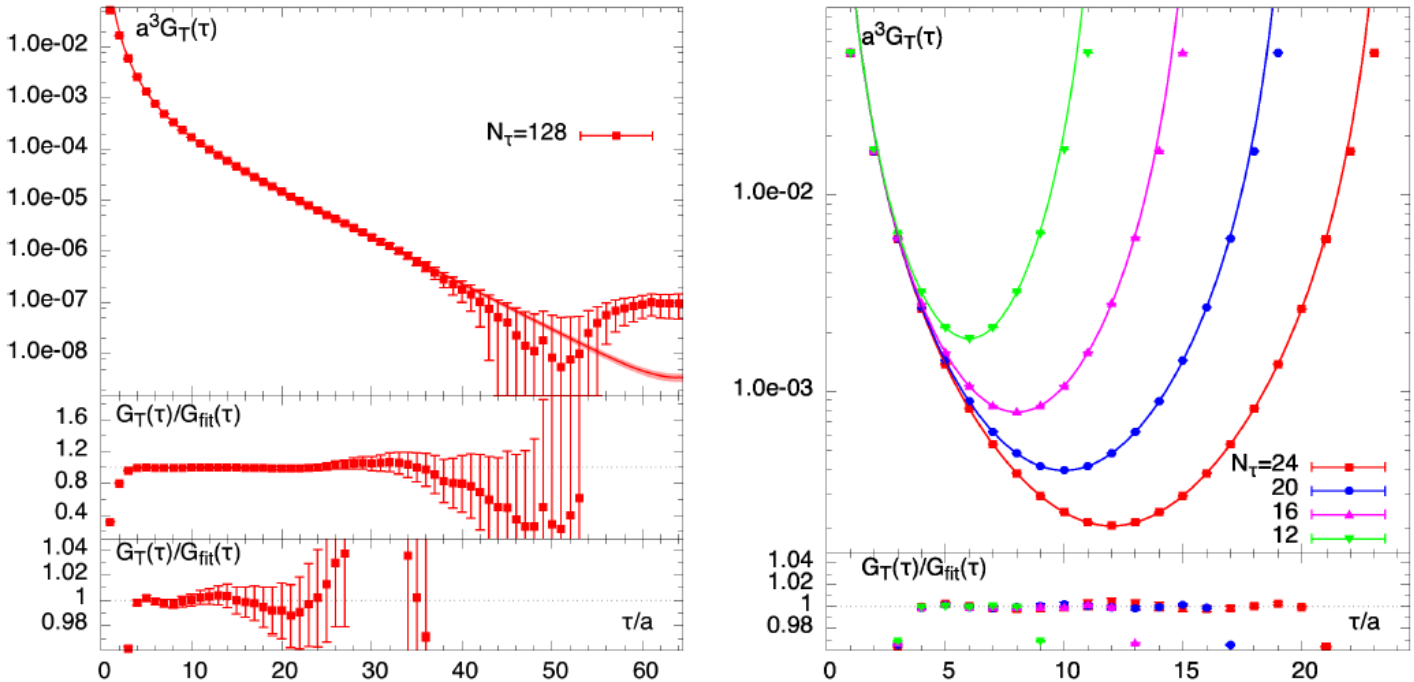

FIG. 1. Left: (Top) The vacuum ($N_\tau = 128$) vector correlation function. The red lines denote the results computed by reconstructing the spectral functions with (Mod. 2c) from the lattice data. The middle panel shows the ratio of the data to the reconstructed result, the bottom panel shows a zoom of this ratio. We observe the lattice data is reproduced with a precision better than 2% for the distance region $\tau/a \lesssim 20$. Right: (Top) The thermal vector correlators at $T/T_c = 0.8, 1.0, 1.25$ and 1.67, i.e. $N_\tau = 24, 20, 16$ and 12. The lines denote the results of the fits based on parametrizing the spectral functions (Mod. 2c). The bottom panel shows the ratio of the data to the fitted correlators.

[B.B. Brandt, A. Francis, B. Jaeger, H.B. Meyer, arXiv: 1512.07249]

Direct comparison of MEM, BGM and SPM - preliminary - Lattice

- Comparison of the reconstructed spectral functions obtained from MEM, Backus-Gilbert and the Schlessinger point method.

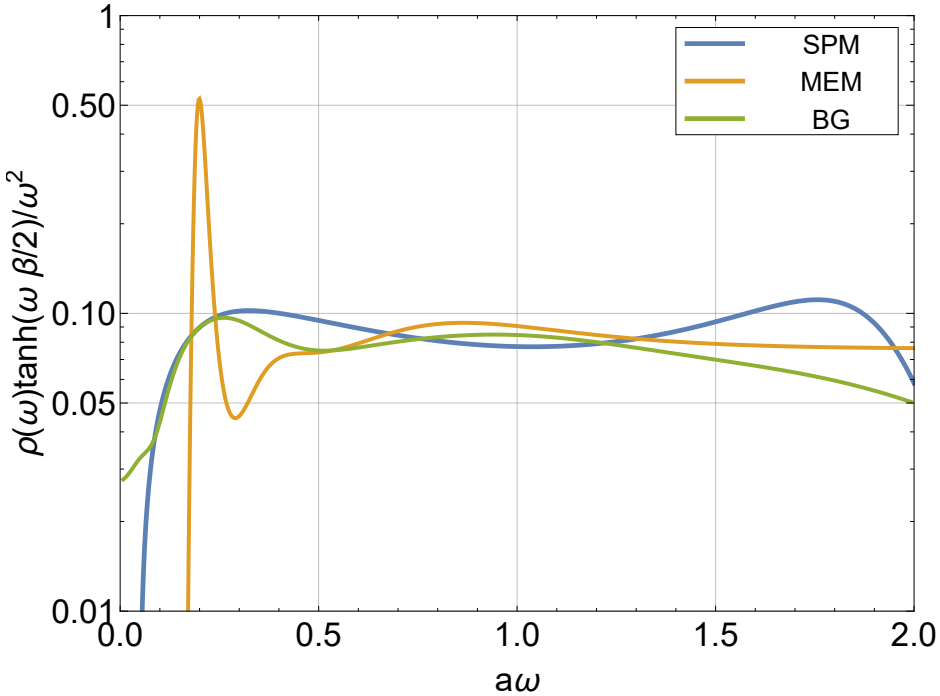

[R.-A. T., P. Gubler, M. Ulybyshev and L. von Smekal, in preparation]

Summary

Rational interpolants computed with the Schlessinger point method (SPM) or Thiele's interpolation function (TIF) can be used to obtain the analytic continuation of a function that is given as numerical data.

- one can reconstruct the underlying function not only along the real axis but also in the complex plane
- can be used to identify resonance poles and to predict decay thresholds (branch cuts)
- can be used to perform an analytic continuation based on Euclidean data